Hindawi
Geofluids
Volume 2022, Article ID 7190994, 25 pages
https://doi.org/10.1155/2022/7190994

Research Article

Origin and Circulation of Springs in the Nangqen and Qamdo Basins, Southwestern China, Based on Hydrochemistry and Environmental Isotopes

Xiwei Qin,[1,2,3] **Haizhou Ma**,[2,3] **Xiying Zhang**,[2,3] **Xiasong Hu**,[1] **Guorong Li**,[1] **Huaide Cheng**,[2,3] **Jibin Han**,[2,3] **Yongshou Li**,[2,3] **Weiliang Miao**,[2,3] **Wenhua Han**,[2,3,4] **Sha Yang**,[1] **Qian Song**,[1] **and Mei Wu**[1]

[1]*Department of Geological Engineering, Qinghai University, Xining 810016, China*
[2]*Key Laboratory of Comprehensive and Highly Efficient Utilization of Salt Lake Resources, Qinghai Institute of Salt Lakes, Northwest Institute of Eco-Environment and Resources, Chinese Academy of Sciences, 810008 Xining, China*
[3]*Key Laboratory of Salt Lake Geology and Environment of Qinghai Province, Qinghai Institute of Salt Lakes, Northwest Institute of Eco-Environment and Resources, Chinese Academy of Sciences, 810008 Xining, China*
[4]*University of Chinese Academy of Sciences, 100049 Beijing, China*

Correspondence should be addressed to Xiwei Qin; 495975224@qq.com

Received 8 June 2021; Revised 30 August 2021; Accepted 2 December 2021; Published 6 January 2022

Academic Editor: Maurizio Barbieri

Copyright © 2022 Xiwei Qin et al. This is an open access article distributed under the Creative Commons Attribution License, which permits unrestricted use, distribution, and reproduction in any medium, provided the original work is properly cited.

The Nangqen and Qamdo (NQ-QD) basins in China have very rich geothermal and brine resources. The origin and spatiotemporal evolutionary processes of its hot and saline springs however remain unclear. Geochemical and isotopic (^{18}O, ^{2}H, ^{3}H) studies have therefore been conducted on the water from the geothermal and saline springs in the NQ-QD Basin. All saline springs in the study area are of the Na-Cl geochemical type while geothermal waters show different geochemical types. The oxygen and hydrogen isotopic compositions of the springs in the NQ-QD Basin are primarily controlled by meteoric water or ice-snow melt water and are influenced by rock-water interactions. It is found that the saline springs in the study area are derived from the dissolution of halite and sulfate that occur in the tertiary Gongjue red bed, while the hot springs in the QD Basin are greatly influenced by the dissolution of carbonatites and sulfates from the Bolila (T_3b) and Huakaizuo (J_2h) formations. Results from silica geothermometry and a silicon-enthalpy hybrid model indicate that the apparent reservoir temperatures and reservoir temperatures for the hot springs in the QD Basin range from 57–130°C to75–214°C, respectively. Deuterium analysis indicates that most of the hot springs are recently recharged rain water. Furthermore, the saline springs have a weaker groundwater regeneration capacity than the hot springs. Tritium data shows that the ranges of calculated residence times for springs in this study are 25 to 55 years, and that there is a likelihood that hot springs in the QD Basin originated from two different hydrothermal systems. The geochemical characteristics of the NQ-QD springs are similar to those of the Lanping-Simao Basin, indicating similar solute sources. Thus, the use of water isotope analyses coupled with hydrogeochemistry proves to be an effective tool to determine the origin and spatiotemporal evolution of the NQ-QD spring waters.

1. Introduction

Hot and saline springs usually refer to springs that form due to the emergence of geothermal resources or saline minerals from the earth's crust. Geothermal resources can provide clean green energy and have recently received considerable attention. To further the understanding of such resources, spring waters can provide significant information about evaporite deposits and geothermal processes in the subsurface because of their halite dissolution and thermal conductivity. The Nangqen-Qamdo (NQ-QD) saline basin was formed as part of the Neo-Tethys Ocean. The basin contains

many evaporite deposits (halite, gypsum, aragonite, dolomite, and magnesite deposition) and saline springs [1, 2], and it is rich in geothermal resources which are mainly distributed in Dingqing, Chaya, Basu, Zuogong, Markam, and Qamdo counties.

The research on underground brine and hot water before 2010 is limited to the exploration stage [3, 4], while the research after 2010 has focused mainly on geological, geophysical, and geochemical data that discuss potassium prospecting, heat sources, and the distribution of hot ground water [5–11]. Only a few studies have used isotopic characteristics to examine the solute source of subsurface brine in the study area [7, 8]. Further, detailed hydrochemistry and isotopic characteristics have rarely been described to assist in understanding the origin and spatiotemporal evolution process of hot and saline springs in the study area. The aim of this study is, therefore, to better describe the genesis, circulation, reservoir temperature, residence time, and spatiotemporal evolution of the hot and saline springs in the NQ-QD basins of China using new hydrogeochemical and water isotope techniques.

The hydrochemistry of springs is widely used to indicate the solute sources, reservoir temperatures, and equilibrium states of groundwater [12–14]. These factors largely control the thermoenergetics potential for a geothermal system. Stable hydrogen and oxygen isotopic ratios are excellent tracers for determining various physicochemical processes in the ground water systems, such as the source of the water and solutes, and the ground water circulation routes (including recharge, runoff, and discharge) [15–19] and describe the rock-water interactions [20, 21]. Tritium (^{3}H), with a half-life of 12.32 years [22], is a naturally occurring radioactive isotope of hydrogen. As tritium is quite stable and not affected by geochemical or biological reactions [23, 24], it can be used to identify mean transit times (MTTs) of modern recharge within the last 50 years [25–28]. The annual average tritium concentrations in prebomb years (before 1952) of meteoric water has decayed to levels below usual detection limits, but it peaked at 6,000 TU in the summer of 1963-1964 because of atmospheric nuclear testing between 1952 and 1970 [26, 29, 30]. Tritium can therefore be used to distinguish pre- and postbomb groundwater recharge. Some studies have focused on the recharge, water and solute sources, transit times, circulation and evolution of ground water, potassium prospecting, and geothermometry of the study area, by assessing the hydrochemistry and analyzing the isotopes of the geothermal waters and the brines (δD, δ^{18}O, and ^{3}H), which not only occur in China, for example, in the Tibetan plateau, Yunnan Province, Tarim Basin and Qaidam Basin [19, 31–34] but also abroad, for example, in the Goa and Tural-Rajwadi geothermal area in India, Hawaii, and California in America and NW Iran [35–39]. The approaches followed in the international examples are therefore applicable in our studies to better understand the origin and circulation of saline and hot springs.

In this study, hydrogeochemical and isotopic characteristics using δD, δ^{18}O, and ^{3}H of saline, hot spring, and river samples collected from the Nangqen and Qamdo basins are analyzed to better understand the circulation depth, recharge sources, residence time, renewability, and hot-cold water mixture ratio of spring waters. The results of this study are also compared to results from certain springs in the surrounding area (Lanping-Simao Basin, Tengchong-Baoshan-Lancangjiang zone, and Yangbajing geothermal field).

2. Geology and Tectonic Setting

The Nangqen Basin (32°00′ ~32°40′N, 96°00′ ~97°00′E) is a Cenozoic lacustrine sedimentary basin, situated in the eastern Qinghai-Tibetan plateau between the Jinshajiang suture and the Nujiang suture. It is a typical shearing-extensional basin, formed by the collision of the Eurasian and Indian plates during the middle Eocene, 45~50 Ma ago [40, 41], resulting in lithospheric shortening and thickening. The NW–SE elongated Nangqen basin, about 55 km long and 18 km wide [42], is part of the Sanjiang fold system [43]. To the west, it is bordered by Carboniferous and Permian organic limestone, to the east by a thrust fault, which is in contact with late Triassic limestone [44]. The sedimentary age of the Nangqen Basin is roughly Late Eocene to Early Oligocene. Stratigraphic development is relatively complete, and it is formed by a set of extremely thick stratified grayish to purplish-red continental clastic rocks containing evaporites, carbonates, and mudstones, accompanied by large-scale high-potassium volcanic rocks [45, 46]. Tertiary Gongjue red sandstone conglomerate and gypsum beds are widely present within the basin. These red beds are overthrust by late Triassic limestone in the eastern part, and the late Triassic limestones are unconformably overlain by Gongjue red beds in the western parts of the basin [47] (Figure 1). The high-K_2O volcanic rocks of the Nangqen Basin include latites, tephrites, trachytes, shoshonites, tephriphonolites, and phonotephrites [48], which belongs to the shoshonitic series and which have been formed by partial melting of an enriched mantle source [49, 50].

The Qamdo basin (29°00′ ~32°00′N, 96°00′ ~99°30′E) is a typical composite back-arc and foreland basin, the back-arc basin of late Paleozoic age, and the foreland basin of Mesozoic age [51, 52]. The basin is located in the east of the Qamdo-Qiangtang block. The Qamdo basin, about 370 km long and 60 km wide, is bordered in the west by the northern Lancangjiang deep fault and in the east by the Ningxia-Deqin deep fault and extends along an NW–SE direction from the Nangqen Basin in the north to Markam County in the south. The basin has experienced several stages of frequent sea-land changes, multiple tectonic movements, and volcanic activities, including (1) a late Paleozoic back-arc basin stage, (2) an early-middle Triassic uplift-denudation stage, (3) a late Triassic sea-level fluctuation stage, (4) a Jura-Chalky atrophy stage, and (5) a Cenozoic extrusion and strike-slip stage [53, 54]. The northern section of the Qamdo Basin (Qamdo area) has a relatively large degree of denudation, which is mainly characterized by quartzitic sandstone, siltite, shale, calcarenitic dolomite, and bioclastic limestone from the Upper Triassic to Jurassic, and is partly dominated by sandstone, siltite, gypsum,

Age	Formation	lithologic description	Thickness (m)	Basin evolution	Sedimentary facies
Tertiary	Lawula (N_2I)	Acidic-neutral volcanics and fuchsia,variegated tuffaceous sandstone	>1083	Himalaya strike-slip pull-apart basin	alluvial, terrestrial and lacustrine facies
	Gongjue (E_{2-3})g	Continental red clastic rock and evaporites	>389		
Cretaceous	Hutousi(K_2h)	Mudstone, siltstone, quartz feldspar sandstone and conglomerate	>985	Yanshan Period Foreland basin formation and developmental stage	terrestrial lacustrine-fluvial facies
	Nanxin(K_2n)		1345		
	Jingxing (K_1j)	Mudstone, argillaceous siltstone and sandstone are interbedded	762-2765		
Jurassic	Xiaosuoka (J_3x)	Quartz sandstone, lithic quartz sandstone, siltstone, shale and paleosol are interbedded	1500-2400		fluvial-lacustrine-delta facies
	Huakaizuo (J_2h)	Argillaceous limestone and gypsum along the Lancang River	358-800		marine-delta-lacustrine facies
	Tutuo (J_1t)	Shale, silty shale with interbedded lithic quartz fine sandstone and siltstone	1636		
	Chalangga (J_1ch)	Lithic quartz sandstone and quartz sandstone	772		Terrestrial fluvial-lacustrine facies
Triassic	Duogaila (T3d)	Shale, arkose quartz sandstone, siltstone with interbedded carbonaceous shale, coal line and coal seam	390		Neritic-delta facies
	Adula(T_3a)		569		
	Bolila (T_3b)	Arenaceous clastic dolomite, pelitic dolomite and arenaceous clastic organisms micrite	300-800		Neritic-terrace facies
	Jiapila (T_3j^2-T_3j^1)	Conglomeratic quartz grit sandstone, conglomerate, feldspar-quartz sandstone and siltstone	732		neritic-lacustrine-fluvial facies
	Walasi (T_2w)	Slate, sandstone and conglomerate, which interbeded with andesiporphyrite, andesitic tuff and a small amount of limestone in the lower-middle strata	2600	Hercynian-Indochina period; back-arc basin developmental stage	
	Malasongduo (T_1m)	Volcanic ash breccia, rhyolite, tuff and sandstone, shale	0-520		

(a)

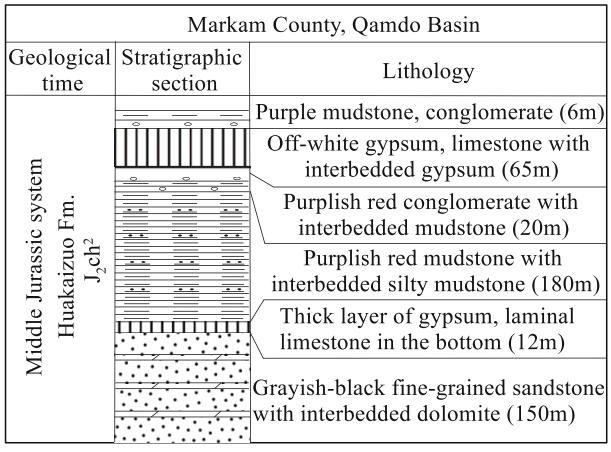

(b)

Figure 1: Continued.

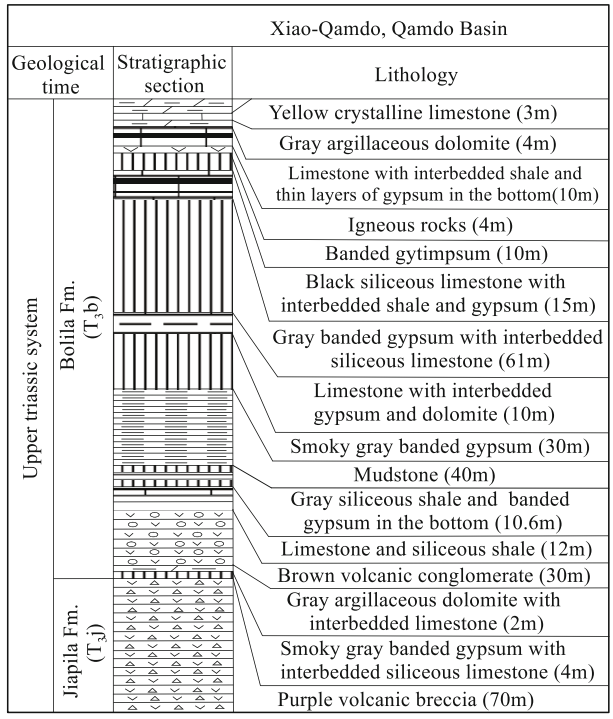

(c)

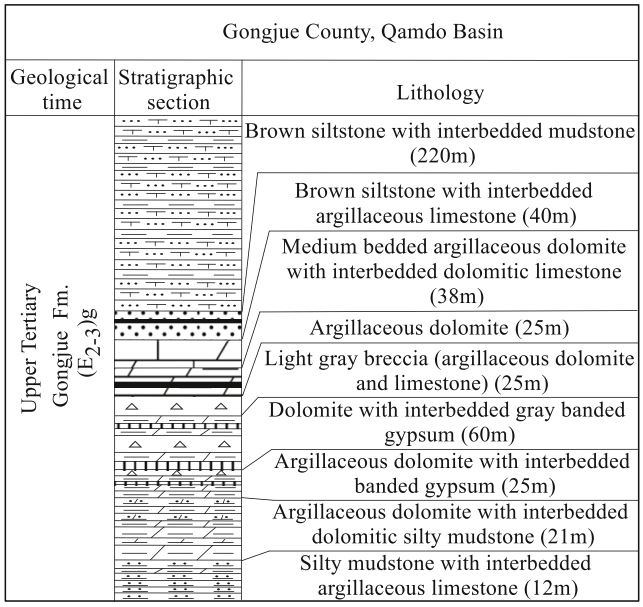

(d)

Figure 1: Continued.

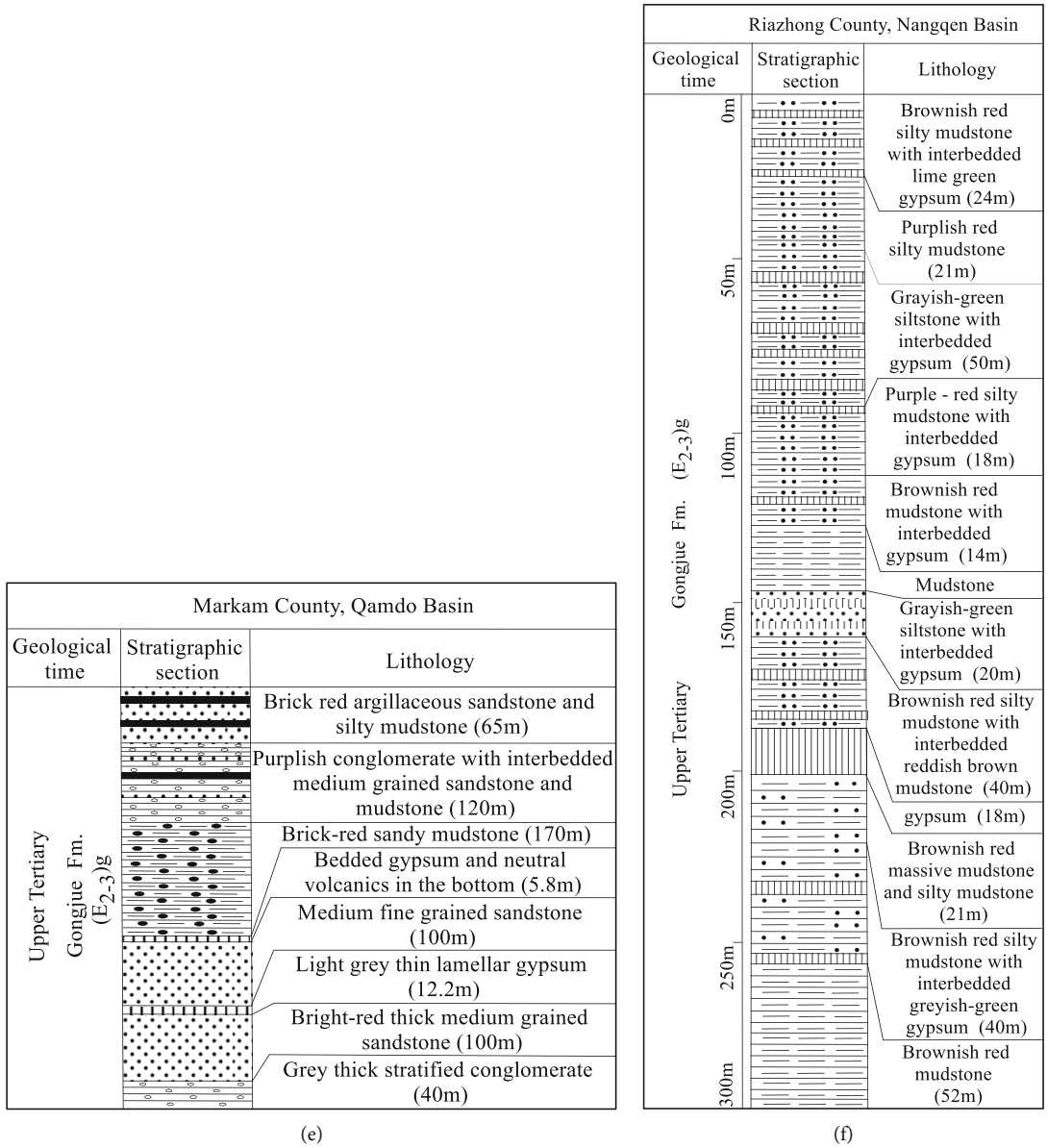

Figure 1: (a) Sedimentary formations and tectonic foundation of the Nangqen-Qamdo Basin (NQ-QD). (b) Lithological sequence of Huakaizuo Formation in Markam County, Qamdo Basin. (c) Lithological sequence of Jiapila and Bolila Formation in Xiao-Qamdo, Qamdo Basin. (d) Lithological sequence of Gongjue Formation in Gongjue County, Qamdo Basin. (e) Lithological sequence of Gongjue Formation in Markam County, Qamdo Basin. (f) Detailed lithological log of the 300 m-thick Ria Zhong section in the Nangqen Basin, Qinghai, China.

argillaceous limestone, and Gongjue red beds (evaporites) ranging in age from the Cretaceous to the Paleogene. The Mesozoic strata in the southern part of the Qamdo basin (Markam area) are well preserved from Jurassic to Paleogene, being especially characterized by Calcareous-bioclastic limestone and gypsum along the Lancang River near the Yanjing and Yuzhong areas [55] (Figure 1).

In this study, chemical and isotopic characteristics were measured in saline and hot springs from the Nangqen and Qamdo basins, and our comparative study includes saline springs from the Lanping-Simao Basin and hot springs from the western Yunnan geothermal belt and the Yangbajing geothermal field. The Yangbajing geothermal field (29°38′-30°20′N, 90°20′-91°35′E) has the highest reservoir temperature of all the Chinese hydrothermal systems and belongs to the Mediterranean–Himalayan geothermal belt. Yangbajing is located about 90 km northwest of Lhasa City, the capital of Tibet. The geothermal field has two reservoirs of different depths: a shallow one (180-280 m) and a deep one (950-1850 m) [56, 57]. The western Yunnan geothermal belt (21°00′-26°00′ N, 96°00′-102°00′ E) can be divided into the Tengchong block, the Baoshan block, and the Lancangjiang zone from west to east. The lithology of these areas is mainly characterized by Gaoligong pluton complexes, muddy limestone, sandstone, granite batholiths, and metamorphic rocks, while the Lancangjiang zone and the Tengchong block

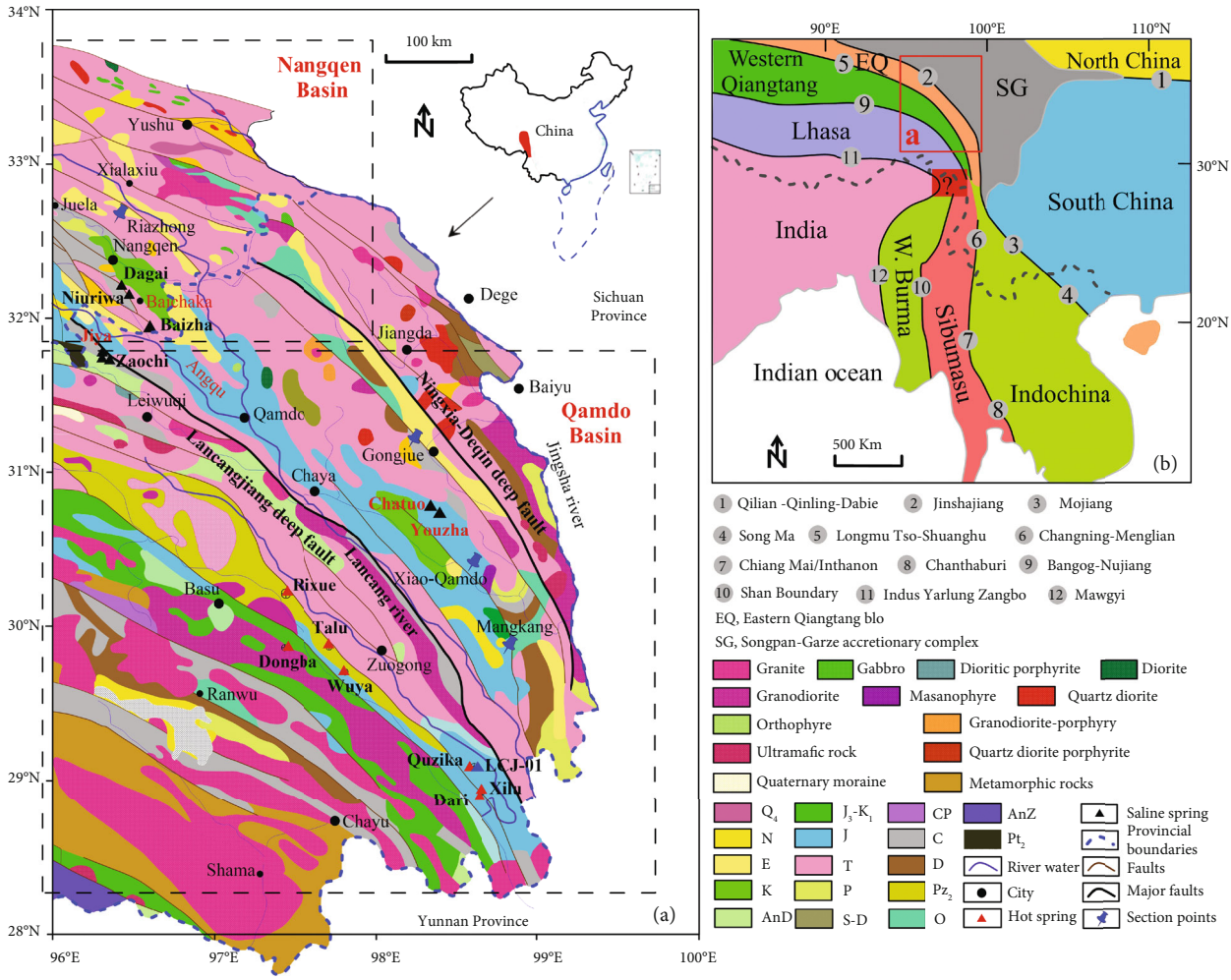

Figure 2: (a) Geological outcrop map and sampling sites in the Nangqen-Qamdo Basin (NQ-QD). (b) Distribution of principal continental blocks and sutures of Southeast Asia [63, 64].

are the main geothermal areas in the western Yunnan geothermal belt [58–60]. The Lanping-Simao Basin is divided by Jingdong to the north for the Lanping sub-Basin (25°00′-29°00′N, 99°00′-101°00′ E) and to the south for the Simao sub-Basin (23°00′-25°00′N, 100°30′-102°30′ E). Red beds with interbedded evaporates are well developed in the Jurassic–Eocene strata [61, 62]. The saline spring solutes in this study mainly originate from Tertiary Gongjue red beds (gypsum, argillaceous limestone, and halite), while the hot springs in Qamdo basin are strongly influenced by Mesozoic strata from the Upper Triassic to Jurassic (Figure 1).

3. Sampling and Analytical Methods

Twenty-seven water samples including 9 saline springs, 13 hot springs, and 5 river water sites were collected from the NQ-QD Basin during the spring (April) of 2019 to obtain their hydrochemistry, $\delta^{18}O$&δD, as well as ^{3}H values. Hot springs are decided to use the first term for water with a sampling temperature of at least one Celsius degree above human body temperature (37°C), that is, approximatively 29.4°C above the mean annual air temperature of the region. The sampling sites are marked in Figure 2. They were filtered through a filter membrane and then transferred into enclosed and cleaned (rinsed with distilled water at least three times) polyethylene bottles for hydrochemical and isotopic analysis.

All water samples were sent to the Salt Lakes Analytical and Testing Department, Qinghai Institute of Salt Lakes, Chinese Academy of Sciences (ISL CAS) for chemical analysis. Chemical analysis of Ca^{2+}, Mg^{2+}, K^{+}, Na^{+}, Li^{+}, Sr^{2+}, and B^{3+} was acidified after collection through the addition of Suprapur HNO_3 to bring the pH below 2 and which was performed by inductively coupled plasma optical emission spectrometry (ICP-OES; IPIS Intrepid II XSP, Thermo Elemental, Madison, WI, USA) with an analytical error of <±1%. Cl^{-}, SO_4^{2-}, and Br^{-} were measured using ion chromatography (using the IC; Dionex 120, Dionex, Sunnyvale, CA, USA) with an analytical error of <±5%. HCO_3^{-} and CO_3^{2-} were determined by hydrochloric acid titration, with an uncertainty of <±1%.

The deuterium (δD) and oxygen-18 ($\delta^{18}O$) isotope analyses were performed at the Analytical Laboratory

Table 1: Geochemical analysis of the surface waters, saline, and hot springs of the Nangqen and Qamdo basins.

Samples	Sample type	pH	T(°C)	TDS	Na^+	Ca^{2+}	Mg^{2+}	K^+	Li^+	Sr^{2+}	B	Si	Cl^-	HCO_3^-	SO_4^{2-}	F^-	Br^-	NO_3^-
					g/L					Mg/L				g/L			Mg/L	
ZC-02	Saline spring	6.7	13.5	76.34	27.94	1.13	0.26	152.00	1.50	20.90	1.59	9.50	43.70	0.36	2.76	5.11	3.42	1.42
DG-01	Saline spring	7.1	12.1	316.74	122.44	1.11	0.18	160.90	8.00	23.10	7.36	17.30	187.45	0.08	5.25	12.05	0.52	1.15
NRW-01	Saline spring	6.6	10.7	313.92	121.14	1.14	0.26	267.30	10.50	27.10	5.17	20.10	186.28	0.12	4.62	9.86	0.04	26.45
NRW-02	Saline spring	6.5	10.4	32.26	12.12	0.27	0.07	85.90	2.80	15.00	4.97	4.00	18.73	0.09	0.87	8.68	0.02	2.39
BZ-02	Saline spring	6.3	11.7	233.88	90.15	1.01	0.16	173.10	8.60	29.00	10.44	4.80	138.76	0.14	3.41	6.07	1.60	9.24
YZ-01	Saline spring	6.7	10.7	37.29	12.51	1.34	0.12	82.30	2.10	29.20	3.08	68.10	19.29	0.18	3.64	8.88	0.02	2.66
CT-01	Saline spring	6.1	11.5	40.24	12.59	2.14	0.29	88.40	2.30	49.00	1.49	26.90	21.63	0.15	3.25	8.71	0.01	13.08
JY-01	Saline spring	7.1	12.3	31.67	10.62	0.89	0.11	670.50	8.80	35.00	14.22	124.10	18.09	0.36	0.74	9.92	0.95	5.32
JY-03	Saline spring	7.1	12.6	33.33	11.22	0.92	0.12	712.40	9.70	39.20	12.83	53.90	19.19	0.32	0.72	6.80	0.99	5.69
YZ-02	Youzha river	8.1	12.1	0.39	0.01	0.07	0.01	7.92	<0.01	1.08	0.46	3.20	0.01	0.17	0.10	2.18	0.00	1.38
JQ-01	Jiqu river	8.3	5.2	0.55	0.05	0.07	0.03	5.00	0.06	2.32	0.20	2.46	0.06	0.22	0.11	2.58	0.00	3.55
ZC-01	River	8.1	6.1	1.68	0.41	0.09	0.05	8.78	<0.01	2.92	0.14	5.00	0.65	0.23	0.22	2.46	0.03	2.68
LCJ-01	Lancang river	8.4	7.0	0.39	0.02	0.06	0.02	5.42	<0.01	0.62	1.35	8.48	0.03	0.16	0.09	1.81	0.03	2.77
LCJ-02	Lancang river	8.4	7.0	0.45	0.03	0.07	0.02	5.32	<0.01	0.48	0.36	2.72	0.04	0.16	0.12	2.28	0.02	3.57
XL-01	Hot spring	7.3	55.3	2.26	0.44	0.19	0.04	23.88	0.70	6.14	1.87	30.42	0.27	0.46	0.80	2.64	0.02	2.57
XL-02	Hot spring	7.4	54.5	2.23	0.43	0.18	0.04	23.32	0.70	5.36	1.91	41.06	0.27	0.45	0.78	3.77	0.02	4.02
DR-01	Hot spring	7.8	53.1	2.34	0.26	0.34	0.07	24.56	0.52	8.92	1.27	17.42	0.23	0.25	1.12	3.94	0.01	4.71
DR-02	Hot spring	7.6	45.2	2.38	0.26	0.35	0.07	25.24	0.48	8.50	1.45	15.40	0.23	0.26	1.16	3.65	0.01	3.00
JY-02	Cold spring	6.7	12.7	0.65	0.09	0.02	0.04	14.74	0.26	<0.0001	0.68	6.70	0.02	0.44	0.02	2.51	0.00	6.01
JY-04	Cold spring	6.7	12.1	1.72	0.41	0.12	0.04	12.52	0.18	1.56	0.84	17.86	0.61	0.20	0.32	2.70	0.00	2.24
TL-01	Hot spring	7.4	60.7	0.98	0.21	0.03	0.01	21.20	0.30	0.76	4.30	30.88	0.02	0.56	0.09	3.33	0.06	0.24
QZK-01	Hot spring	8.4	78.8	0.43	0.10	0.01	0.00	9.48	0.36	0.26	1.81	22.86	0.02	0.22	0.04	14.79	0.05	0.34
QZK-02	Hot spring	8.5	54.6	0.32	0.06	0.02	0.00	7.20	<0.01	1.30	0.54	14.40	0.01	0.16	0.03	7.53	0.03	4.35
WY-01	Hot spring	7.3	77.1	1.49	0.36	0.03	0.00	19.50	0.86	1.78	3.96	28.20	0.02	0.99	0.03	3.65	0.04	0.25
WY-02	Hot spring	7.3	77.1	1.51	0.36	0.03	0.01	22.30	0.86	1.06	4.30	26.78	0.03	0.99	0.03	5.42	0.00	6.44
RX-01	Hot spring	7.5	40.5	1.16	0.25	0.03	0.01	29.40	0.98	1.10	6.35	19.64	0.04	0.64	0.11	9.04	0.00	2.58
DB-01	Hot spring	7.1	45.3	0.40	0.02	0.05	0.02	4.72	<0.01	0.36	0.52	7.78	0.01	0.25	0.03	2.97	0.00	1.11

Table 2: Field observations, locations, water types, and isotope date of the surface waters, and saline and hot springs in the Nangqen and Qamdo basins.

Sample name	Location	Elevation (m)	Water type (Schukalev's classification)	T(°C)	pH	$\delta D_{V\text{-}SMOW}$	$\delta^{18}O_{V\text{-}SMOW}$	*d* value	TU	Std err
ZC-02	N31°43′59.0″ E096°	3743	Na-Cl	9.5	7.67				3.4	±0.7
DG-01	N32°12′15.0″ E096°	4061	Na-Cl	11	7.8	-127.39*	-14.52*	-11.23	1.9	±0.7
NRW-01	N32°08′38.7″ E096°	3700	Na-Cl	10.5	7.11	-124.14*	-14.38*	-9.1	1.3	±0.4
NRW-02	N32°08′38.7″ E096°	3700	Na-Cl	10.5	7.15					
BZ-02	N31°56′02.6″ E096°	4087	Na-Cl	8.5	7.05	-132.98*	-16.00*	-4.98	2.7	±0.7
YZ-01	N30°44′05.0″ E098°	3787	Na-Cl	12.1	7.34	-134.9	-17.3	3.5	5.5	±0.8
CT-01	N30°47′05.0″ E098°	3660	Na-Cl	11.7	7.12	-134.7	-17.3	3.7	<1.3	
JY-01	N31°46′26.0″ E96°	3782	Na-Cl	14	7.15	-125.8	-16	2.2	6.9	±0.8
JY-03	N31°46′26.0″ E96°	3782	Na-Cl	15.1	7.2					
YZ-02	N30°44′9.0″ E98°	3708	Na-Cl	12.1	7.2					
JQ-01	N31°40′9.1″ E96°	3556	Ca-Mg-Na-HCO_3	11.2	7.55					
ZC-01	N31°43′18.7″ E96°	3619	Ca-Na-Mg-HCO_3	9.7	7.47	-119.2	-15.2	2.4		
LCJ-01	N29°5′20.3″ E98°	2259	Na-Cl	16	8.34				4.1	±0.7
JY-02	N31°46′26.0″ E96°	3782	Na-Mg-HCO_3	15	7.31					
JY-04	N31°46′26.0″ E96°	3782	Mg-Na-Cl	14.5	7.52					
XL-01	N28°55′47.6″ E98°	2201	Na-Ca-SO_4-Cl	54.2	7.3				3	±0.5
XL-02	N28°55′47.6″ E98°	2201	Na-Ca-SO_4-Cl	51.5	7.5	-131.9	-18	12.1		
DR-01	N28°53′55.7″ E98°	2194	Ca-Na-SO_4	45	7.8	-116.7	-15.7	8.9	2.8	±0.6
DR-02	N28°53′56.7″ E98°	2172	Ca-Na-SO_4	42	7.7					
TL-01	N29°52′24.9″ E97°	3992	Na-HCO_3	47	7.6	-159.5	-20.6	5.3	<1.3	
QZK-01	N29°5′33.0″ E98°	2276	Na-HCO_3	75	8.51	-131.4	-18.1	13.4	<1.3	
QZK-02	N29°5′ 33.7”E98°	2297	Na-Ca-HCO_3	78	8.65					
WY-01	N29°42′11.3″ E97°	3785	Na-HCO_3	65	8.2	-161.1	-20.8	5.3	<1.3	
WY-02	N29°42′11.3″ E97°	3785	Na-HCO_3	70	8.1					

Table 2: Continued.

Sample name	Location	Elevation (m)	Water type (Schukalev's classification)	T(°C)	pH	$\delta D_{V\text{-}SMOW}$	$\delta^{18}O_{V\text{-}SMOW}$	*d* value	TU	Std err
RX-01	N30°13′2.6″ E97°	3812	Na-HCO_3	42	7.6	-156.5	-20	3.5	<1.3	
DB-01	N29°51′31.7″ E97°	3327	Ca-Mg-Na-HCO_3	62	7.8	-150.3	-20.2	11.3	1.5	±0.5
Riazhong saline spring	N32°15′15.1″ E96°	3759	Na-Cl	10.5	6.84	-128.28*	-14.68*	-10.84		
Duolunduo saline spring	N32°04′48.5″ E96°	3837	Na-Cl	11.9	7.54	-100.91*	-12.88*	2.13		
Ranmu saline spring	N32°26′43.1″ E95°	4374	Na-Cl	6.1	6.98	-128.36*	-16.05*	0.04		
Gayang saline spring	N32°03′47.9″ E95°	4225	Na-Cl	12	7.05	-129.57*	-15.93*	-2.13		
Naxi saline spring	N29°02′51.0″ E98°	2588	Na-Cl	10.5	7.58	-107.6	-12.8	-5.2		

*Data from saline springs in the Nangqen Basin were obtained from [7].

Beijing Research Institute of Uranium Geology (ALBRIUG PRC). The δD and δ^{18}O values were determined by water-gas equilibration method at MAT 253 stable isotope ratio mass spectrometer (Thermo Scientific, USA), and the results are reported relative to SMOW with an analytical precision of ±2‰ and ±0.2‰, respectively. Tritium was analysed by an electrolytic enrichment method followed by a liquid scintillation counter (Perkin Elmer 1220c Quantulus) with an analytical precision of 0.12 TU ($\pm 1\sigma$ criterion) and was carried out at the Analytical Laboratory Beijing Research Institute of Uranium Geology [35, 65–67]. Tritium water samples were collected in 500 mL clean high-density polyethylene bottles of which 250 mL of the water were distilled. The distilled sample was then enriched by electrolysis at a low temperature (1 ~ 4°C). Finally, the enriched sample was mixed with a scintillation cocktail and put into a liquid scintillation counter with a very low background (Perkin Elmer 1220c Quantulus). The results are denoted by TU (tritium units), where 1 TU = 0.12 Bq/l.

4. Results

Chemical and isotopic data of spring waters from the NQ-QD Basin are listed in Tables 1 and 2. The spring waters had a wide range of salinities (32.74~327.44 g/L for saline springs, 0.33-2.43 g/L for hot springs, and 0.4-1.72 g/L for river waters). The cations and anions for saline springs in the Nangqen and Qamdo basins fall near to the Na + K and Cl endmembers, respectively (Figure 3), which have similar chemical characteristics, with Na + K > Ca > Mg and Cl > SO_4 > HCO_3. The chemical concentrations of the hot springs are relatively consistent (Na + K > Ca > Mg for cations, HCO_3 > SO_4 > Cl or SO_4 > HCO_3 > Cl for anions), except for Dongba (Ca > Na + K > Mg). For river waters, Ca is the main cation (Ca > Na + K > Mg), and HCO_3 is the main anion (HCO_3 > SO_4 > Cl) (except for Zaochi). The Piper diagram shows five water types for the hot springs in the Qamdo Basin, including (1) Na-HCO_3 (Quzika-01, Rixue, Talu, Wuya), (2) Ca-Mg-Na-HCO_3 (Dongba), (3) Na-Ca-HCO_3 (Quzika-02), (4) Ca-Na-SO_4 (Dari), and (5) Na-Ca-SO_4-Cl (Xilu). All saline springs in the Nangqen (Baizha, Niuriwa) and the Qamdo basins are of the Na-Cl type, except Jiya-03 (which has a Mg-Na-Cl signature). The Lancang river in Markam is of the Ca-Mg-Na-HCO_3 or Ca-Na-Mg-HCO_3 type. The δD values range from -161.1 to -116.7‰ for hot springs and from -134.9 to -107.6‰ for saline springs. The δ^{18}O values of the hot springs range from -20.8 to -15.7‰, whereas the saline springs range from -17.3 to -12.8‰. The isotope composition greatly influences the water isotope results for hot and saline springs, especially for high salinity springs, which are characterized by mineral dissolution and cold water mixtures [68–70]. The tritium content for the hot and saline springs varies from <1.3 to 3.0 TU and from 1.3 to 6.9 TU, respectively, except for the Chatuo hot spring.

The classical Gibbs diagram (Figure 4) shows that the saline springs' chemical composition is dominated by evaporation crystallization processes because all the data points plot on the evaporation crystallisation end member, similar to the composition of seawater and saline springs from the Lanping-Simao Basin (Figure 4). The chemical composition of the hot springs in the study area is primarily controlled by rock weathering and evaporation of atmospheric precipitation-dominated water, which is partially influenced by evaporation. Most of the data points of the surface waters plot on the intermediate area between the rock dominance end member and the evaporation/precipitation dominance end member (Figure 4). This indicates that the water chemistry of the Lancang and Tajiqu rivers may be a product of rock-water interaction and evaporation, while

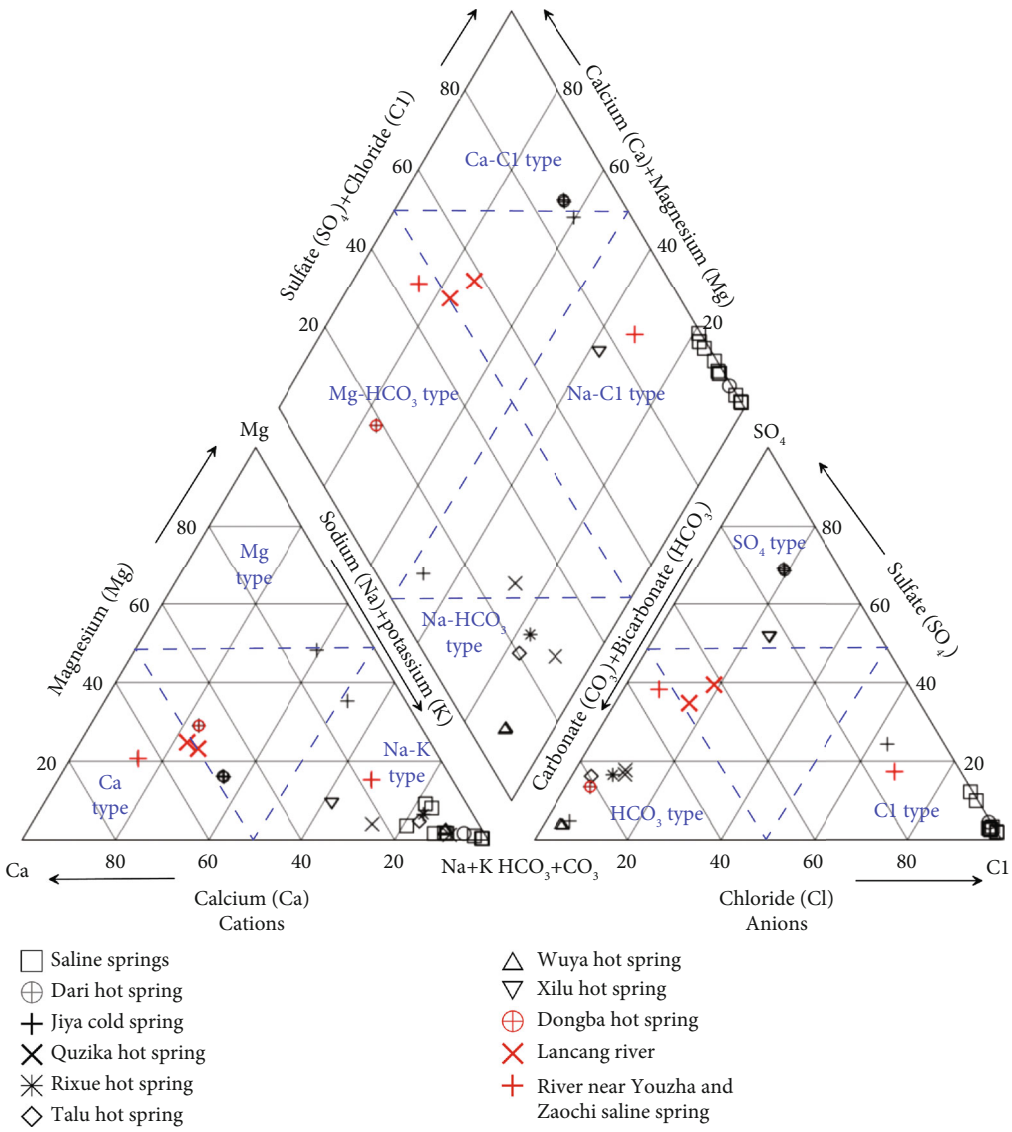

Figure 3: Piper diagram of the saline and hot springs in the Nangqen and Qamdo basins (NQ-QD). All concentrations are in mg/L.

the water chemical composition of Jiqu, which is situated in Jiqu Township, Nangqian County, is mainly controlled by evaporation. Most geothermal waters from western Yunnan plot on the rock dominance endmember revealing water that is dominated by rock-water interactions. Geothermal waters from Yangbajing plot on the intermediate area between the rock dominance end member and the evaporation dominance end member indicating that rock dissolution and evaporation are the dominant processes controlling the major ion composition of geothermal waters from Yangbajing. Apart from precipitation and evaporation, rock-water interaction is the most important factor controlling the chemical composition of natural waters, which is greatly influenced by the formation lithology. Saline springs are mainly influenced by the dissolution of evaporate (gypsum and halite rocks), and hot springs are influenced by the carbonatite and gypsum in the Mesozoic strata, while geothermal waters from Yangbajing and western Yunnan are influenced by the granitic batholiths and metamorphic rocks.

5. Discussion

5.1. Recharge Source and Circulation of Spring Waters

5.1.1. Evidence-Based on $\delta^{18}O$ and δD Values. $\delta^{18}O$ and δD values can be used as an excellent tracer of various physicochemical processes in groundwater systems. They provide key information on the fluid origin and recharge, rock-water interaction, water contamination, evaporation, and mixing rates [17, 72–75]. From the $\delta^{18}O$-δD plot (Figure 5), it is seen that all the spring samples collected from the Nangqen and Qamdo basins fall near the global meteoric water line (GMWL) [17], the China meteoric

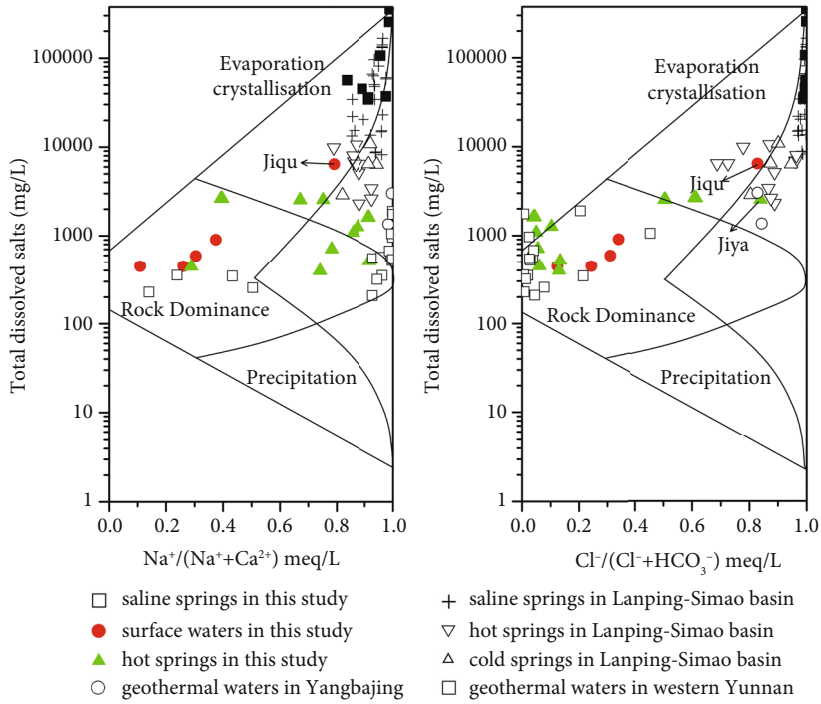

Figure 4: Gibbs plots indicating the mechanisms controlling the saline and hot springs' water chemistry [31, 34, 57, 71].

water line (CMWL), and the Southwest China meteoric water line (SW CMWL) [76]. However, the saline springs in this study slightly deviate from the meteoric water line due to the strong evaporation and intense rock-water interactions, as evidenced by the Na-K-Mg and Gibbs plots (Figures 4 and 6(a)). This suggests that all the hot and saline springs mainly originate from meteoric water, but saline springs in this study may experience deeper water circulation, more intense rock-water interaction, and more extensive evapoconcentration, compared to meteoric water. Figure 5 reveals a deviation in ^{18}O concentrations for the Wuya, Talu, and Rixue hot springs. This deviation is because of oxygen exchange from meteoric waters to rock minerals during high-temperature hydrolithogenesis, which results in higher $\delta^{18}O$ values in the water and lower $\delta^{18}O$ values in rocks.

The rainwater-dominated spring water can be assumed to be mainly composed of glacial meltwater and modern rainwater because the NQ-QD Basin is located in the northern Hengduan Mountains, with an average elevation of more than 3500 meters, and has perennial snow cover. A binary mixing model was used to estimate the relative contributions of glacial meltwater (MW) and modern precipitation (PPT) to spring waters in the study area. The mixing model was calculated using the formula: $\delta^{18}O_{\text{springs}} = f_{\text{mw}}\delta^{18}O_{\text{mw}} + f_{\text{ppt}}\delta^{18}O_{\text{ppt}}$, where f_{mw} and f_{ppt} are the fractions of springs originating from glacial meltwater and modern precipitation in the study area, of which the total value is 1. Because saline springs in this study have shown slight $\delta^{18}O$ deviations, this mixing model is suitable for hot springs in Qamdo basin. The $\delta^{18}O_{\text{mw}}$ and $\delta^{18}O_{\text{ppt}}$ values are represented by the $\delta^{18}O$ value of glacial meltwater (-20.74‰) from the mountain pass between Zuogong and Rongxi [77] and modern precipitation (-16.9‰) from the Chaya county [78]. The resulting estimated proportions of glacial meltwater in hot springs ranged from 29% to 96%, while one hot spring (Wuya) had no modern precipitation contribution.

The stable isotopic composition of precipitation exhibits an obvious altitude effect [79–81], which means that the isotopic gradient can be used to infer the recharge areas of the aquifers [82]. All the hot and saline spring samples are located along the LMWL and display a good linear correlation on the δD vs. $\delta^{18}O$ chart ($R^2 = 0.87$). The isotope data (δD and $\delta^{18}O$) follow a linear relationship with altitude, which can be expressed by the regression lines $Y = -395.92x - 4461.19$ ($R^2 = 0.75$) ($\delta^{18}O$ for hot springs), $Y = -317.92x - 1562.0$ ($R^2 = 0.76$) ($\delta^{18}O$ for saline springs), $Y = -46.01x - 3537.79$ ($R^2 = 0.89$) (δD for hot springs), and $Y = -41.64x - 1787.50$ ($R^2 = 0.77$) (δD for saline springs), respectively (Figure 7). This indicates that hot and saline springs originate from local precipitation. Field observations prove that the river water originates in rainfall or snow-melt water in high mountainous areas, but the large Lancang river and Angqu river are not the main recharge sources of the hot and saline springs. The rivers only seem to serve as discharge conduits because the hot springs are much more depleted in δD and $\delta^{18}O$ isotopes than those of the Lancang River water, while many hot springs develop along the river from the upper reaches to the lower reaches of the rivers [55], which indicates that river water does not infiltrate deep into the geothermal reservoirs and is not the recharge source of hot springs [83]. The Tibetan Plateau is covered with ice and snow all year round, and the

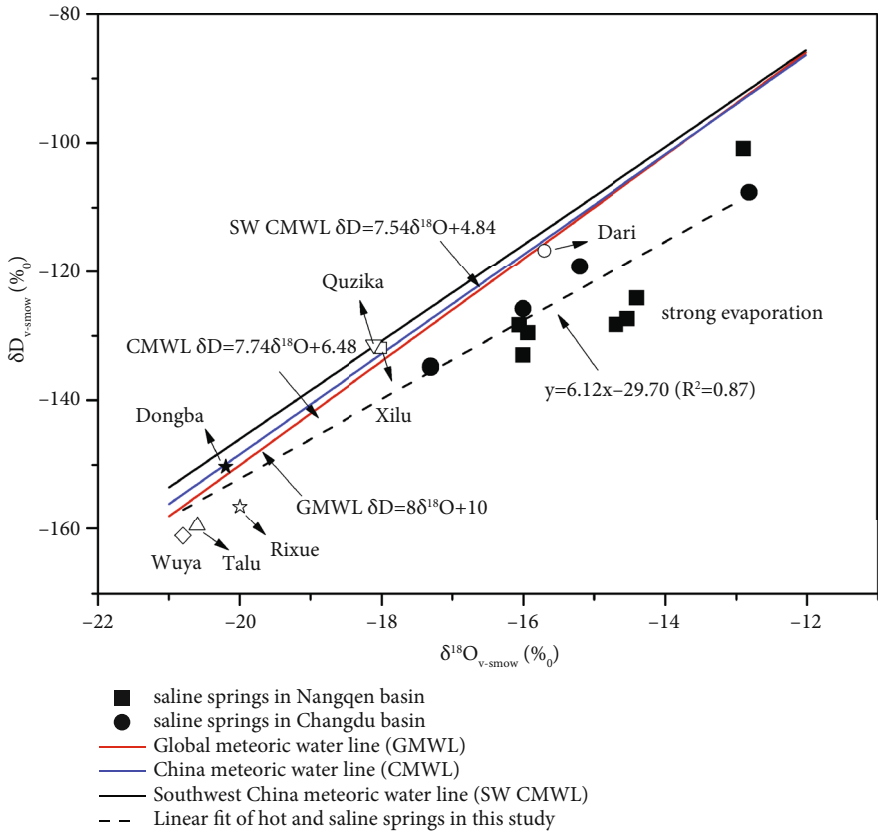

Figure 5: Isotope composition (δD and δ^{18}O) of the saline and hot springs in the Nangqen and Qamdo basins plotted against the GMWL, the CMWL, and the SW CMWL.

recharge elevation of the springs is approximately equal to the snow line. The summer weather is warm and humid, causing the snow line to move up and the ice to melt. Under the action of gravity, the melt water circulates along deep faults which are mainly caused by the uplift of the Tibetan Plateau. Furthermore, there is no deep hydrothermal recharge in the study area. If river waters were to serve as the main recharge source for hot springs, no such large-scale high pressure large flux geothermal eruptions would exist because the elevation from source to discharge are similar. Local people have also observed an increase in hot spring fluxes in the study area in recent decades. This could be caused by an increase in melt water on the Tibetan Plateau due to global warming in recent decades. The melt water or rainfall in the northern Hengduan Mountains can therefore be the main recharge sources of hot springs along the Lancangjiang deep fault.

The relationship between δ^{18}O & δD and the elevation for meteoric water in eastern Tibet, western Sichuan, and Guizhou can be expressed by the equation $-\delta^{18}O\,(‰) = 0.0031H\,(m) + 6.19$ and $-\delta D\,(‰) = 0.026H\,(m) + 30.2$, respectively, where H is the recharge elevation (m). This indicates that the isotopic gradient is independent of the hot and saline springs and the recharge elevations of the hot and saline springs can be estimated by the isotopic gradient. The δD values are relatively stable during high temperature hydrolithogenesis due to the low hydrogen content in the rock minerals; so, they can be used to calculate the recharge altitude in this study. The calculated recharge elevation of the springs in the Nangqen and Qamdo basins is as follows: 2720~3953 m (average = 3628 m) for the Nangqen saline springs, 2977-4027 m (average = 3625 m) for the Qamdo saline springs, and 3327-5034 m (average = 4374 m) for the Qamdo hot springs. The estimated recharge elevations of the hot springs in the Qamdo basin, using δ^{18}O as a tracer, range from 3170 to 4870 m (average = 4151 m). The ~200 m overestimation in the inferred recharge altitude of the hot springs by δ^{18}O tracers can be attributed to the δ^{18}O deviation because of the rock-water interaction and strong evaporation. The Nangqen and Qamdo basins are located in the northern Hengduan Mountains (above 4000 m), which are close to the mean altitudes of the saline and hot spring waters, which indicates that the hot and saline springs are mainly derived from meteoric water or ice-snow melt water from the northern Hengduan Mountains. By contrast, springs sampled at elevations of ~3700 m for the Qamdo saline springs, ~2300 m for the Yanjing Town saline springs, and~3100 m for the hot Qamdo hot springs, are lower than the recharge elevation of the study area, being located ~500 m lower for saline springs, and more than 1000 m lower for the hot spring. The long vertical distance between the recharge area and the discharge area may drive the rapid and deep circulation of the spring waters under the action of gravity.

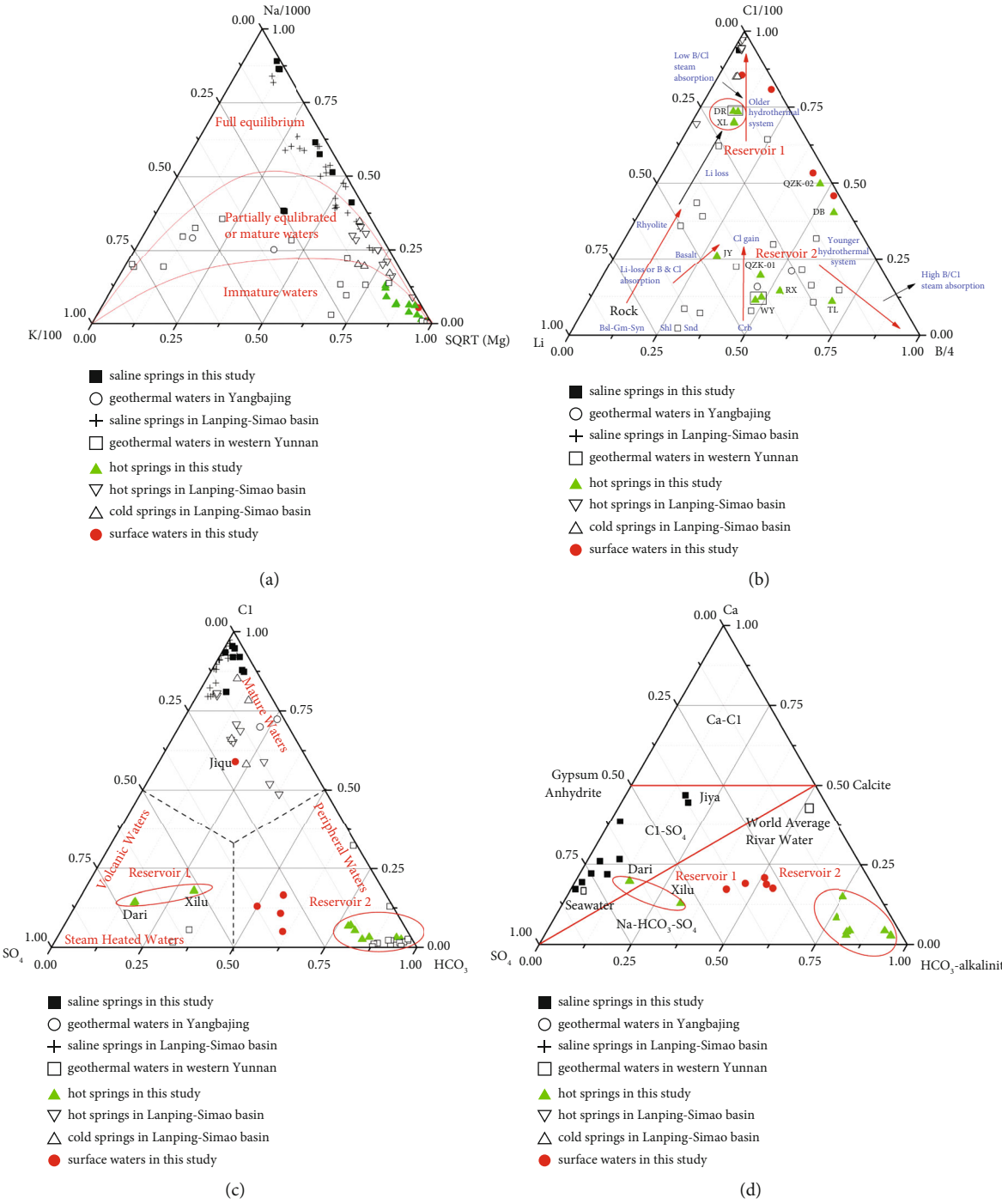

FIGURE 6: Ternary phase diagram, modified from [96] for the saline and hot springs in the Nangqen and Qamdo basins, where *a* denotes the Na-K-Mg plot, *b* denotes the Cl-Li-B plot, *c* denotes the Cl-SO_4-HCO_3 plot, and *d* denotes the Ca-SO_4-HCO_3 plot.

The depth of the spring water circulation (Z_{circ}) can be estimated by the following formula: $Z_{circ} = (T_r - T_0/Grad\ T) + Z_0$ (for the hot water system) and $Z_{circ} = 2T_s - T_0/GradT$ (for the cold-hot water mixed system), The average geothermal gradient (GradT) is about 3°C/100 m in the study area, and the mean annual air temperatures and the temperature of initial cold water, T_0, for the Nangqen and Qamdo basins, are 7.6°C and 4.4°C[55], T_r and T_s are the reservoir temperature and the outlet temperature of the hot springs in study area, respectively, and the depth of the constant-temperature zone (Z_0) is 20 m. The mixing of cold water with deep thermal water that is moving up through the formations (Figure 7) is represented by the mixed system formula. Different temperatures for the hot springs can be used in the mixed system formula to calculate the circulation depth of the hot springs. The estimated circulation depth of the hot springs in this study ranges from 2495 m to 5002 m.

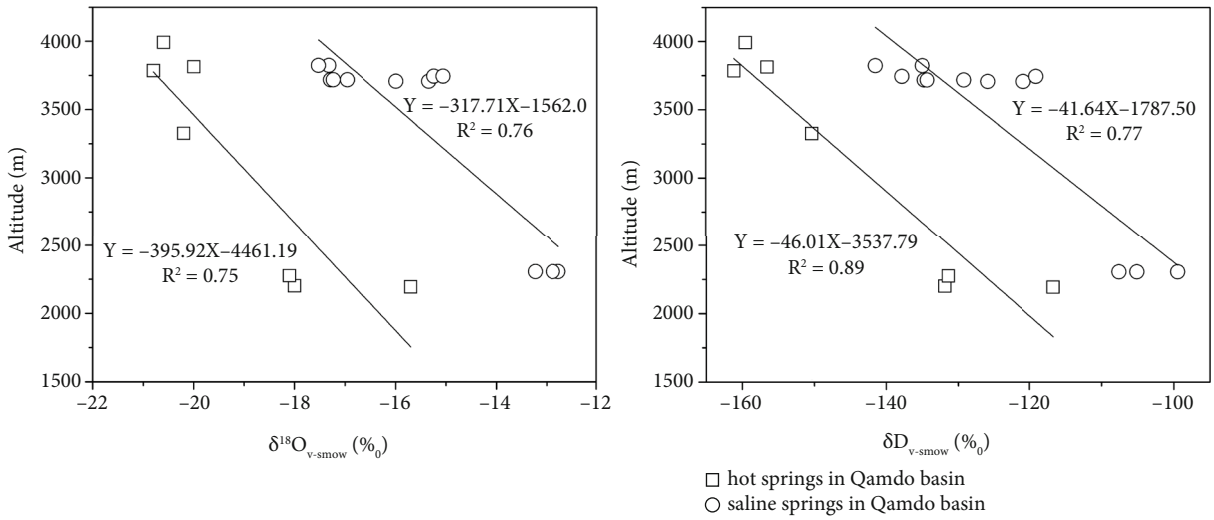

Figure 7: Relationships between $\delta^{18}O$ and altitude and δD and altitude for the hot and saline spring waters in the Qamdo Basin.

5.1.2. Evidence-Based on Deuterium Excess Parameter. The d value comprehensively reflects the degree of exchange of the local rock-water oxygen isotopes and also represents the degree of deviation from modern atmospheric precipitation, which is defined as $d = \delta D - 8\delta^{18}O$ [80]. A $d < 10\%$ indicates normal atmospheric precipitation, while a $d < -10\%$ indicates that atmospheric precipitation was subjected to evaporation and concentration, and a $d > +10\%$ indicates precipitation that differs from current climatic conditions [84]. The d value for cold springs in the study area varies from -11.23 to 13.4 (average = 1.59), while the d value for hot springs in the Qamdo basin varies from 3.5-13.4 (average = 8.54). For saline springs in the Nangqen Basin, the d value varies from -11.23-2.13 (average = −5.16), and for saline springs in the Qamdo basin, the d value varies from -5.2-3.7 (average = 1.32). Most of the springs may therefore have originated from normal atmospheric precipitation, but the hot springs of Xilu, Quzika, and Dongba in the Qamdo basin and the saline springs of Dagai and Riazhong in the Nangqen basin may however have derived from atmospheric precipitation that differs from current climatic conditions. The saline springs of Dagai and Riazhong may have experienced stronger evapoconcentration than the other springs.

5.2. Solute Sources and Genesis of Spring Waters

5.2.1. Hydrochemistry Evidence. The ratios of the hydrochemical characteristics (such as the nNa/nCl, nCa/nMg, $100nSO_4/nCl$, nMg/nCl, and Br ×103/Cl ratios) are of great importance for understanding the genetic type and occurrence environment of groundwater. The nNa/nC1 ratio (or metamorphic coefficient) represents the degree of stratigraphic sealing. If the nNa/nC1 ratio of groundwater is larger than the standard seawater value (0.85), it means that groundwater is influenced by the infiltration of meteoric water, and that the geothermal system is relatively open. The nCa/nMg ratio exhibits positive correlations with the residence time and degree of metamorphism of the deep groundwater, and a higher ratio indicates that the strata have better sealing properties. Generally, if the nCa/nMg ratio of underground water is greater than 3, it represents a more closed geothermal system. The redox environment of groundwater can be measured by the $100nSO_4/nCl$ ratio (the desulfurization coefficient), which can be used to evaluate the degree of sealing of the groundwater storage environment. Generally, if the $100nSO_4/nCl$ ratio > 10.26 (the standard seawater value), it indicates a weak desulfurization acid and a relatively open groundwater storage environment. The nNa/nCl, nCa/nMg, and $100nSO_4/nCl$ ratios from the hot springs in the Qamdo Basin display very large variations, ranging from 1.04 to 23.05 (with an average of 8.25), from 0.35 to 5.96 (with an average of 2.96), and from 19.17 to 193.4 (with an average of 100.5), respectively. The nNa/nCl and $100nSO_4/nCl$ ratios of the hot springs in this study were greater than 0.85 and 10.26, while the nCa/nMg ratios of most hot springs were around 3, except for Quzika hot spring. This can be attributed to infiltration of meteoric water, weaker metamorphism, and a relatively open thermal storage environment in the Qamdo Basin.

The Cl/Br ratio can be used as a tracer to determine the source and evolution of surface water and groundwater with low-to-moderate salinity, as well as to determine the input of salinity in rivers and lakes [85–89]. Present-day seawater exhibits constant Cl and Br concentrations, and its Cl/Br molar ratio of 655 ± 4 (the Br ×103/Cl (g/g) is about 3.44 ± 0.02) [90]. Br is generally not metallogenic by itself; so, it can only stay in the mother liquid based on the isomorphism in the mineral crystal lattice. Br in the brine is often enriched by migration and depleted by dilution, and Mg is preferentially enriched in marine evaporite parent halides during the deposition process. The Br ×103/Cl and the nMg/nCl ratios should therefore be low in leached brines (0.87–0.08 or smaller for Br ×103/Cl and 0–0.16 for nMg/nCl) and high in sedimentary brines [91]. The nNa/nCl ratio denotes the enrichment degree of sodium salt in

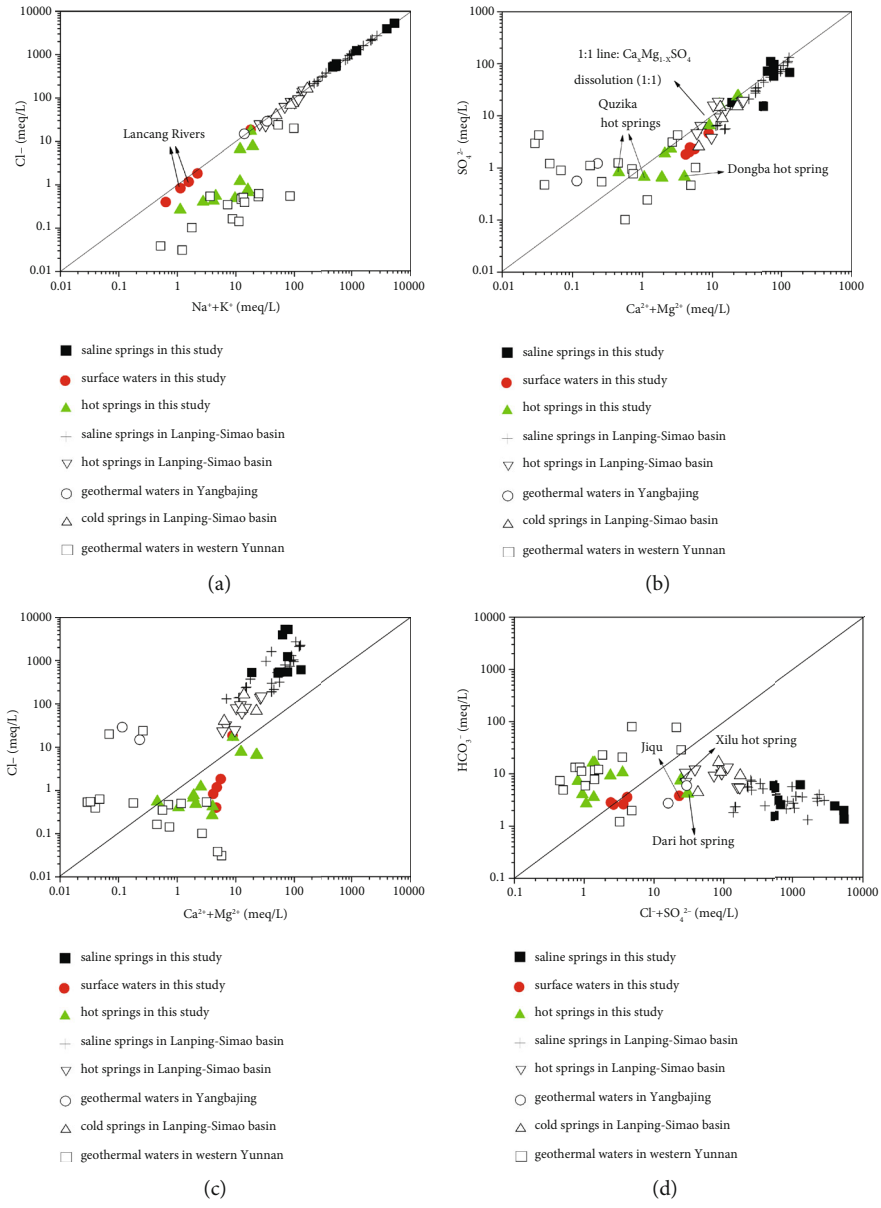

Figure 8: Continued.

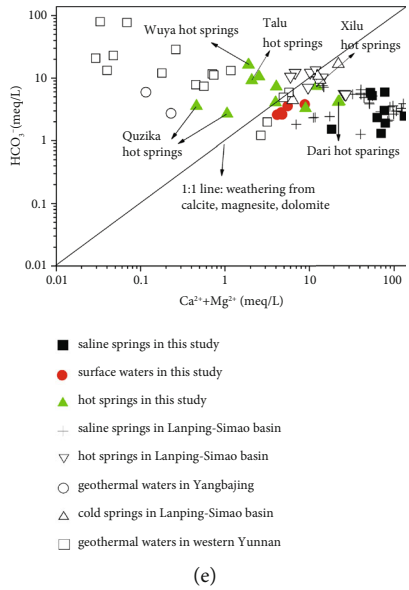

(e)

Figure 8: Plots of (Na + K) vs. Cl, (Ca + Mg) vs. SO_4, (Ca + Mg) vs. Cl, (Cl + SO_4) vs. HCO_3, and (Ca + Mg) vs. HCO_3 in spring waters from the Nangqen-Qamdo (NQ-QD) Basins and the comparative Lanping-Simao Basin study area. All concentrations are in meq/L.

brine, with a boundary of 0.87, and the nNa/nCl ratio in leached brines ranges from 0.87 to 0.99 (≈1) [92]. The approximate 1 : 1 nNa/nCl molar ratio of the saline springs in this study is distinct from hot springs and surface waters. All of the saline springs sampled in our study area have low levels of bromide (0.01–3.42 mg/L). The ratios of Br ×103/Cl (0.0002–0.078), nMg/nCl (0.003–0.039) and nNa/nCl (0.90–1.01) in the saline springs suggest that halite dissolution is the major process that dominates the chemistry of the saline springs in the Nangqen and Qamdo basins. The most likely source of halite is the Gongjue Evaporite Formation, which is interbedded with the Tertiary continental red clastic rocks from which the saline springs emerge and which consists of relatively pure gypsum, argillaceous limestone, and halite [55, 61, 93].

The ion ratio diagrams can further assist in understanding the solute source of groundwater and surface waters. The data for all of the saline springs in this study plotted below the equivalence line (the 1 : 1 line), similar to the saline, hot, and cold springs in the Lanping-Simao Basin (Figure 8(a)). This means that the evaporite is the main material source of the saline springs in this study and not the carbonatite. In the Qamdo Basin, however, HCO_3^- is enriched relative to $Cl^- + SO_4^{2-}$ for most of the hot springs (except for the Dari and Xilu hot springs) (Figure 8(d)), indicating that most hot springs may have derived from the dissolution of carbonatite, similar to the geothermal waters in western Yunnan and the hot springs in Dari and Xilu, which may have diluted the sulfate-bearing strata along both sides of the Lancang River. Figure 8(a) implies that Na^+, K^+, and Cl^- for saline springs in this study and the Lanping-Simao Basin primarily come from the dissolution of halite and sylvine, similar to hot and cold springs in the Lanping-Simao Basin. Dating for most of the hot springs in this study and the geothermal waters in western Yunnan lies far from the equivalence line, indicating that hot springs in this study are not associated with salt rock leaching. From Figure 8(b), combined with Figures 8(e) and 8(c), sulfate is the principle source, and carbonatite is the minor source of Ca^{2+} and Mg^{2+} in saline and hot springs in the study area and the Lanping-Simao Basin because the correlation of (Ca^{2+}+Mg^{2+}) vs. SO_4^{2-} is better than that of (Ca^{2+}+Mg^{2+}) vs. HCO_3^-. The Ca^{2+} in hot springs also correlates positively with Sr^{2+} (average = 2.85 mg/L) and SO_4^{2-} (average = 351.1 mg/L) and has calculated regression lines of $Y = 36.68X + 2.13$ ($n = 13$, $R^2 = 0.93$) and $Y = 136.62X - 38.79$ ($n = 13$, $R^2 = 0.96$), respectively. This may be caused by the interaction of the circulating hot springs with the evaporitic ($CaSO_4$) units, which is confirmed by the wide distribution of Paleogene evaporite strata in the Qamdo Basin. While Ca^{2+} and Mg^{2+} in geothermal waters from Yangbajing and western Yunnan are less relevant to the evaporite or the carbonatite, they may have something to do with the large granitic batholiths and metamorphic reservoir host rocks [34, 71]. The Ca + Mg is enriched relative to HCO_3^- and depleted relative to Cl^- in saline springs from the study area and in the Lanping-Simao Basin, indicating that the dissolution of evaporites (halite, sylvine, and gypsum/anhydrite) is the principal sources of solutes for the saline springs.

The alkali metal Li is not affected by secondary processes and can be used as a tracer for deep rock dissolution processes [94]. Cl^- and B^- are the most conservative constituents in the geothermal system and are fixed in the fluid phase and have not equilibrated; so, the B/Cl ratio and Cl-Li-B ternary diagram are the best geoindicators to evaluate the possible origin of the fluid. Relative Cl^-, B^-, and Li^+ concentrations of the saline and geothermal waters of the study area and the comparative area are compared with rock compositions in Figure 6(b) [94, 95]. Samples from the Dari and Xilu hot springs plotted close to the chloride corner, indicating that these constituents originated in old hydrothermal systems, but other hot

springs in this study may have originated in younger systems. The origin of the Dari and Xilu hot springs implies much larger gains of Cl^- and considerable Li^+ losses, as suggested by the local geological conceptual model, which is characterized by clastic sedimentary rocks and mudstones in the Early to Middle Jurassic. The rock data plots on the axis of the Li^+ and B^+ end elements and the hot springs (Wuya, Quzika, Rixue, and Jiya) that interact with carbonate-evaporite rocks are found below the middle of the ternary phase diagram. The saline springs in the study area and the Lanping-Simao Basin plotted close to the chloride corner (Figure 6(c)) and are classified as mature neutral chloride waters, which are associated with halite dissolution. The Dari and Xilu hot springs plotted in the field between steam-heated waters and volcanic waters, but the hot springs in the study area are neutral to alkaline (7.1-8.5, average = 7.6), which is not consistent with steam-heated waters and are characterized by a low pH. The Dari and Xilu hot springs are therefore likely to be volcanic fluids in which hydrogen sulphide has been oxidized to sulphate, while the other hot springs in this study are thought to be bicarbonate water. Based on Figure 6(d), all the saline springs in the study area plot in the Cl-SO_4 field and the majority of the hot springs in the study area plot in the Na-HCO_3-SO_4 field. The saline springs also plot very close to the HCO_3-end-member, which may indicate that the saline springs mainly form by the dissolution of sulfates and halites in the Paleogene strata, and that most hot springs are closely related to the widely distributed carbonate rocks in the study area of Jurassic and Cretaceous age. The Dari and Xilu hot springs however plot near the chemical divide (the line from calcite to SO_4), which may indicate the addition of meteoric water to the sulfates and carbonate minerals. Surface waters plot in the Na-HCO_3-SO_4 field, meaning that this water mainly derives from meteoric water.

5.2.2. Stratigraphic and Lithologic Evidence. Both limestones/dolomites (from the Late Triassic to Jurassic) and the Tertiary Gongjue red beds (containing gypsum/anhydrite, argillaceous limestone, and halite) are widely present in the Nangqen and Qamdo basins. The Triassic carbonates in the study area belong to the Bolila Formation, which is characterized by arenaceous clastic dolomite, pelitic dolomite, and clastic organisms in the form of micrite [55]. The following reactions describe the dissolution of the calcite (Equation (1)) and dolomite (Equation (2)), where calcite is the dominant mineral in micrite. The dissolution of calcite and dolomite produces the total molar concentrations of Ca^- and Mg^- ions are equal to the concentration of HCO_3^-.

$$CaCO_3 + CO_2 + H_2O \longrightarrow Ca^{2+} + 2HCO_3^-, \quad (1)$$

$$CaMg(CO_3)_2 + 2CO_2 + 2H_2O \longrightarrow Ca^{2+} + Mg^{2+} + 4HCO_3^-. \quad (2)$$

The Ca^{2+} and Mg^{2+} concentrations are more than HCO_3^- of saline springs in the study area, but the hottest spring and surface water samples are located along the 1 : 1 line (Figure 8(e)), which can be explained by the additional dissolution of halite and sulfate-containing minerals in the saline springs, while the hot springs in the Qamdo Basin are mainly dominated by the dissolution of Triassic carbonates and influenced to a lesser degree by gypsum from Jurassic to Paleogene strata along the Lancang River.

Both gypsum and anhydrite are present in the Gongjue Evaporite Formation and the Mesozoic strata of the southern Qamdo Basin along with halite. Gypsum is highly soluble in the presence of calcite or halite that is in solution [97]. The dissolution of gypsum results in equal milliequivalent concentrations of Ca^{2+} and SO_4^{2-} in solution and is expressed by the following reaction:

$$CaSO_4 \bullet 2H_2O \longrightarrow Ca^{2+} + SO_4^{2-} + 2H_2O. \quad (3)$$

Data points are posted along the 1 : 1 line, and correlations between Ca and Sr ($R^2 = 0.93$), SO_4 ($R^2 = 0.96$), are high for hot springs in the Qamdo Basin. This suggests that the dissolution of sulfate minerals contributes to the chemical composition of the saline and hot springs in this study.

5.3. Reservoir Temperature. The Na-K-$Mg^{1/2}$ ternary diagram is commonly used to classify waters into fully equilibrated, partially equilibrated, and immature waters for the application of ionic geothermometers [98–100]. All the hot springs and surface waters in the study area plot in the immature water zone (close to the $Mg^{1/2}$-end-member), while most saline springs in this study and the Lanping-Simao Basin plot in the fully equilibrated water zone and partly equilibrated water zone (Figure 6(a)). This means that rock-water interactions have reached equilibrium for most of the saline springs in this study area, and that reactions between the fluid and the rock were unable to reach equilibrium for hot springs or that the hot springs in this study area may have mixed with surface water or may have been diluted. [101] proposed that the content of conservative elements (e.g., Cl^-) in geothermal water correlate well with $\delta^{18}O$ and δD values and B contents due to the mixing of cold and hot water. All the hot springs in the Qamdo Basin display a good linear correlation between Cl vs. $\delta^{18}O$ and δD values, except for the Xilu and Dari hot springs that do not show a linear Cl-B plot. This means that all of the hot springs experienced mixing with cold water, but that the Xilu and Dari hot springs may be affected by mixing with other water sources (e.g., volcanic fluids).

Some geothermometers are commonly used: cation geothermometers, silica geothermometers, and multimineral equilibrium geothermometers [102]. As each geothermometer can only be used under very specific conditions, it is very important to select the appropriate geothermometer for the intended purpose. Using a cationic thermometer requires fully equilibrated waters, so the cationic thermometer cannot be used in hot springs. The silica geothermometer may be a reasonable choice for hot springs [103], while the silica geothermometer and the multimineral Na–K geothermometers can be used for equilibrated saline

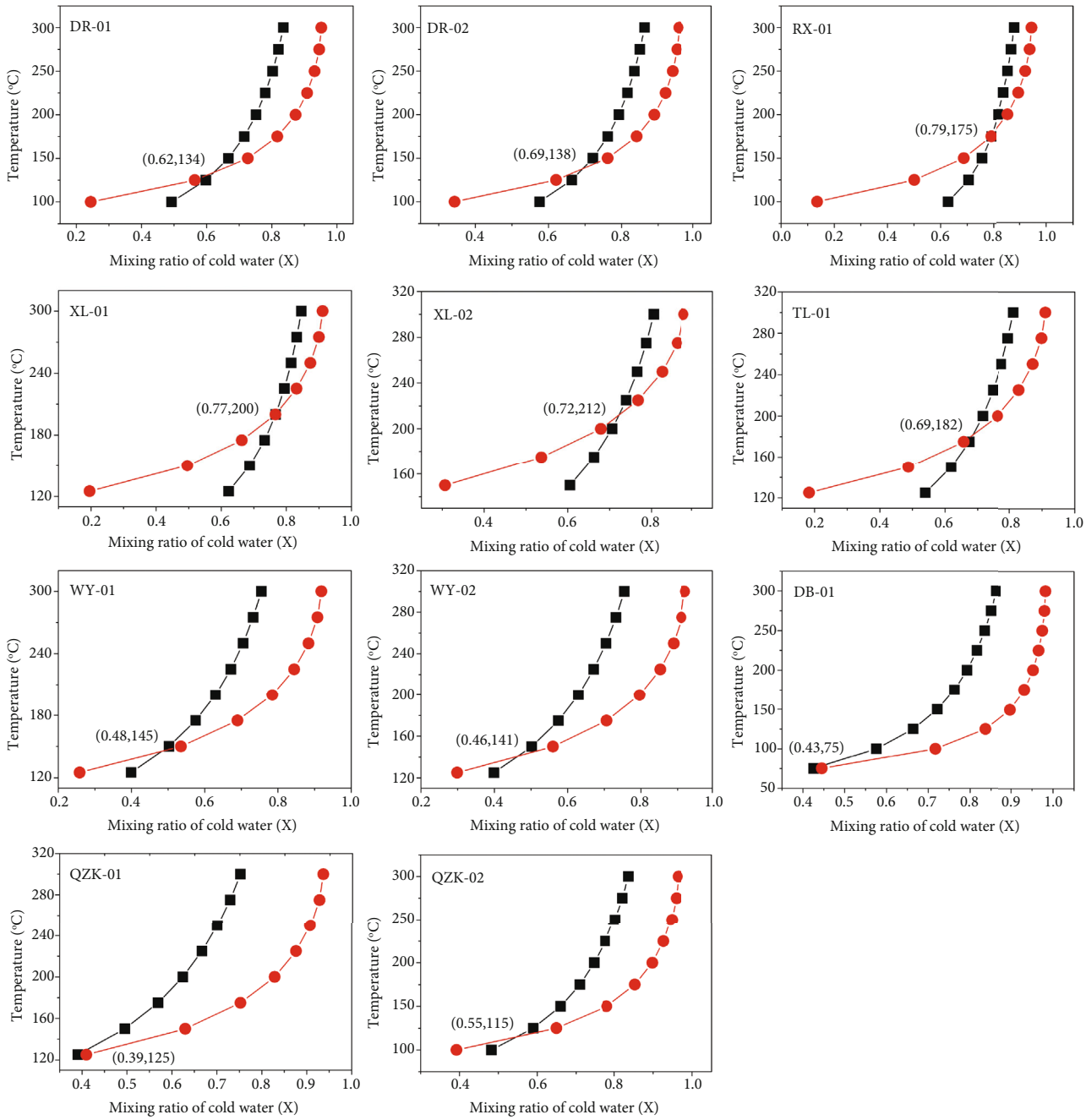

Figure 9: Plot of the mixing ratio vs. the temperature for hot springs in the Qamdo Basin.

springs. Because of mixing with cold water, the reservoir temperature calculated by the silica and multimineral Na–K geothermometers are lower than the real value so, the silicon-enthalpy hybrid model must be used to correctly estimate the geothermal reservoir temperature (Tr).

The Silicon-enthalpy hybrid model to estimate the Tr was calculated using the formulae:

$$\begin{aligned} H_c X + H_h(1-X) &= H_s, \\ SiO_{2c}X + SiO_{2h}(1-X) &= SiO_{2s}, \end{aligned} \tag{4}$$

where H_c, H_h, and H_s are the enthalpy of cold groundwater, the deep thermal groundwater, and the spring water, respectively; SiO_{2c}, SiO_{2h}, and SiO_{2s} are the SiO_2 concentrations of the cold groundwater, the deep thermal groundwater, and the spring water, respectively; and X is the mixing ratio of the cold groundwater, where the estimated mixture ratio of cold groundwater range from 39% to 79% (Figure 9). Four representative formulas for silica thermometer estimation are suggested by [104] that are as follows:

$$T_{\text{Quartz-no}} = \frac{1309}{5.19 - \log(\text{SiO}_2)} - 273.15\,(25 - 250^{\circ}\text{C}),$$

Table 3: Estimated reservoir temperatures of the hot springs in the study area.

Sample ID	Calibration status	SiO_2 (mg/L)	$T_{quartz-no}$	$T_{quartz-max}$	$T_{calibrate\ silicon}$	$T_{chalcedony}$
XL-01	Uncorrected state (cold water mixing effect is not eliminated)	65.2	114.6	113.6	114.9	85.7
XL-02		88.0	130.2	126.8	130.3	102.7
DR-01		37.3	88.7	91.1	89.2	57.8
DR-02		33.0	83.4	86.5	83.9	52.2
TL-01		66.2	115.4	114.2	115.6	86.5
QZK-01		49.0	100.9	101.7	101.3	70.9
QZK-02		30.9	80.6	84.1	81.1	49.3
WY-01		60.4	110.9	110.3	111.2	81.6
WY-02		57.4	108.3	108.2	108.7	78.9
RX-01		42.1	93.9	95.7	94.4	63.5
DB-01		16.7	56.7	63.0	56.6	24.4
		16.7-88.0	56.7-130.2	63.0-126.8	56.6-130.3	24.4-102.7
XL-01	Corrected state (cold water mixing effect is eliminated)	283.4	205.0	188.4	206.2	188.1
XL-02		314.2	213.0	194.8	214.4	197.5
DR-01		98.2	136.2	131.9	136.4	109.4
DR-02		106.5	140.7	135.7	140.9	114.4
TL-01		213.5	184.4	171.8	185.1	164.0
QZK-01		80.3	125.3	122.7	125.5	97.4
QZK-02		68.6	117.1	115.7	117.4	88.5
WY-01		116.2	145.8	139.9	145.9	120.0
WY-02		106.3	140.6	135.6	140.8	114.3
RX-01		200.4	180.1	168.3	180.7	159.0
DB-01		29.2	78.4	82.1	78.9	47.0
		29.2-314.2	78.4-213.0	82.1-194.8	78.9-214.4	47.0-197.5

Calibration status: uncorrected state (where the cold water mixing effect is not corrected for). Corrected state (where the cold water mixing effect is corrected for).

$$T_{Quartz-max} = \frac{1522}{5.72 - \log(SiO_2)} - 273.15\ (25 - 250^{\circ}C),$$

$$T_{Chalcedony} = \frac{1032}{4.69 - \log(SiO_2)} - 273.15\ (0 - 250^{\circ}C),$$

$$T_{Calibrate\ silicon} = -42.198 + 0.28831SiO_2 - 3.6686 \times 10^{-4}(SiO_2)^2 + 3.1665 \times 10^{-7}(SiO_2)^3 + 77.034 \lg SiO_2. \quad (5)$$

The estimated reservoir temperature (Tr) of the hot springs in this study is listed in Table 3. When the cold water mixing effect is not corrected for, the calculated reservoir temperatures using the chalcedony geothermometer (24–103°C) are lower than that of the quartz-no steam loss equation (57–130°C), the quartz-maximum steam loss at 100°C equation (63–127°C), and the calibrate silicon equation (57–130°C). The shallow reservoir temperature (apparent reservoir temperature) of the geothermal system in this study is therefore selected as 57–130°C (Table 3). When the cold water mixing effect is corrected for, the calibrate silicon reservoir temperature (79–214°C) is similar to the calculated reservoir temperatures by the quartz-no steam loss equation (78–213°C) and the quartz-maximum steam loss equation at 100°C (82–195°C), which is higher than that of the chalcedony geothermometer (49–197°C) (Table 3). Based on the calculated results, the reservoir temperature of the geothermal system in this study is regarded as 78–214°C, similar to the value calculated by the silica-enthalpy mixing model (75–212°C), see Figure 9.

5.4. Residence Time of the Spring Waters. Tritium is very mobile and exchanges very easily with hydrogen or water molecules. It exists in various forms, such as the liquid form as HTO, the gaseous form as HT, and in CH_3T as organic bound tritium (OBT) [105]. The tritium radioisotope (3H or T) with a half-life period of 12.32 years is a direct tracer of water movement in predominantly the HTO form in liquid [106]. It can therefore be used to estimate mean transit times (MTTs), groundwater recharge rates and renewability, and the pathway of water in different hydrogeological settings as well as the rates or directions of subsurface flow [105, 107–111]. There are two major sources of tritium in the atmosphere: atmospheric thermonuclear testing tritium (that were produced from 1953 to 1963) and tritium produced by cosmic rays. Atmospheric tritium is controlled by latitude and season [112, 113], and nuclear testing tritium

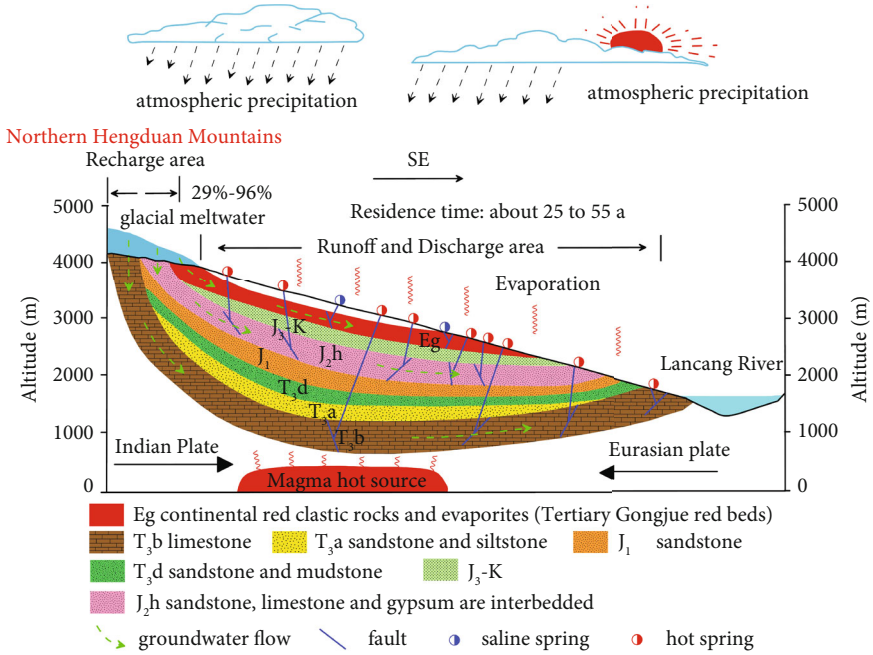

Figure 10: Sketch map of the evolution of springs in the Nangqen-Qamdo Basin.

can be used to discriminate recharge water in terms of modern groundwater or water that recharged before nuclear testing [114].

The tritium content in the groundwater can trace the origin of supplemental water, where a tritium content less than 1 TU can be interpreted as submodern groundwater recharge before 1952, and a tritium content ranging from 1 to 4 TU reflects a mixture of modern and submodern groundwater recharge. The tritium content of the hot springs in this study area appears to be generally low (<4 TU). The highest value recorded is ~3.0 TU for the Xilu hot spring, with most hot springs showing a tritium content below the detection limit (1.3 TU). The hot springs in Talu, Quzika, Wuya, and Rixue can therefore be interpreted as having been recharged by submodern water from before 1952, while the hot springs in Xilu, Dari, and Dongba are dominated not only by submodern water but also by modern water. The tritium content of the saline springs ranges from 1.3 to 6.9 TU, except for the Chatuo hot spring, which has less than 1.3 TU. It can be inferred that most saline springs have been influenced by a combination of modern and submodern water, and that modern water played a larger role than submodern water in the saline springs in Youzha and Jiya.

With atmospheric nuclear tests no longer being carried out, the tritium content in meteoric water has already returned to close to its natural level. The groundwater of different ages and recharge sources may mix under certain hydrodynamic conditions. Mixing of cold surface water and water from shallow thermal reservoirs tend to keep the tritium content of the groundwater relatively high, but the relatively long replenishment and circulation cycles in the groundwater system decrease the tritium content of the groundwater, complicating isotope dating with tritium isotopic in practice. Tritium content in groundwater can however be used to qualitatively estimate age ranges (mean transit times) and groundwater migration processes in geothermal systems [40, 83, 117] because geothermal waters with relatively long replenishment and circulation cycles in the region's deep reservoirs are essentially tritium free or have relatively low tritium levels.

A simple isotopic model can be used to calculate the hot water residence time using the formula $t = \ln({}^3H/{}^3H_0)/-0.056$, where ${}^3H_0$ and ${}^3H$ are the background values and the measured tritium values of the hot springs in TU. Because tritium has a half-life of 12.43 years, so the decay constant (λ) of tritium is equal to 0.056 a^{-1}. The background value of tritium (${}^3H_0$) in this study was chosen as the tritium content of meteoric waters in Lhasa City (28.15 ±1.29 TU). The ${}^3H_0$ values that were below the detection limit (1.3 TU) were taken as 1.3 TU for the estimation of the groundwater residence time. The ranges of the calculated residence time for hot and saline springs are approximately equal (25.1–54.9 years for hot springs and 29.2–54.9 years for saline springs). The background value of tritium (28.15 ± 1.29 TU) calculated in this study is greater than the current natural background value of tritium (10 TU); so, it can be inferred that the water of the springs in this study area has been transported, and that the underground groundwater retention time was at least 6.6-36.4 years.

5.5. Conceptual Model of Spring Water Circulation. The evolution of water resources in the NQ-QD Basin is very complicated, and a conceptual model for the circulation of the spring water in this study is proposed (Figure 10).

With the uplift of the Tibetan Plateau and the retreat of the Tethys Sea, many unique geothermal fields and saliferous strata developed in the NQ-QD Basin. In addition, the NQ-QD Basin contains two groups of northeast and northwest-trending faults stretching tensile active faults, which can serve as favorable conduits for conducting groundwater circulation. The hydrochemistry and water isotopic characteristics of springs indicate the spring waters from the study area originated from leaching and circulation of meteoric water or ice-snow melt water recharge from the northern Hengduan Mountains combined with rock-water interaction. While spring waters flow through the host rocks, which are characterized by evaporates, carbonate rocks, silicate rocks, and volcanic rocks, the geochemical data show that dissolution of evaporates (such as halite and gypsum/anhydrite) in, for example, the Tertiary Gongjue red beds are the principle sources of solutes that control the chemistry and the salinity of the saline springs in this study, whereas the solute sources of hot springs in the QD Basin may mainly be controlled by the dissolution of carbonatites and sulfates from the Bolila (T_3b) and the Huakaizuo (J_2h) formations. The recharge source of groundwater containing soluble mineral components (such as salts, gypsum, and carbonates) leached from host rocks and flows along large fracture zones through which it can penetrate the formation for deep circulation, with a depth ranging from 2494 m to 5005 m for the hot springs. The hot springs may have a stronger groundwater regeneration capacity than the saline springs. This water is then heated by the geothermal system which originates from the magmatic heat source after which further rock-water interaction occurs. Spring waters ascend via faults to the surface of the earth (the discharge area) and then mix with shallow cold groundwater under tectonic and static pressure. Based on tritium concentrations, the calculated residence time for the hot and saline springs ranges from 25 to 55 years to migrate from the recharge area to the discharge.

6. Conclusion

(1) Based on detailed chemical and water isotopic data for O and H, the spring waters in the NQ-QD Basin mainly derive from the leaching and circulation of meteoric water or ice-snow melt water from the northern Hengduan Mountains and are greatly influenced by rock-water interactions. The saline springs in the NQ-QD Basin mainly form due to the dissolution of halites and sulfates in the, for example, the Tertiary Gongjue red beds, which is the most important salt-bearing formation in this region. It is composed of continental red clastic rocks and evaporates that include relatively pure gypsum/anhydrite, argillaceous limestone, and halite. The hot springs in the QD Basin may have derived from the dissolution of carbonatites (limestones/dolomites) from the Late Triassic (T_3b) Bolila Formation and the sulfate-bearing strata along both sides of the Lancang River from the Jurassic (J_2h) Huakaizuo Formation. The hydrochemical characteristics of the springs in the NQ-QD Basin are similar to those of the Lanping-Simao Basin but differ from spring waters collected from the western Yunnan geothermal belt and the Yangbajing geothermal field, suggesting that solute sources are similar between NQ-QD springs and Lanping-Simao springs

(2) Because the water from the hot springs in this study mixes with surface water and may be diluted, the apparent reservoir temperature and actual reservoir temperature in the Qamdo geothermal system are calculated using silica geothermometry and the silicon-enthalpy hybrid model. These two methods yielded reservoir temperatures of 57–130°C and 75–214°C, respectively. Based on the tritium concentrations and the deuterium excess parameters, saline springs in this study are considered to have a more closed hydrogeological environment and experiences less groundwater recharge than hot springs, where the calculated residence time for the hot and saline springs range from 25 to 55 years

(3) Based on the calculated reservoir temperatures and ternary phase diagram, the circulation depths of the hot springs in the QD Basin are predicted to range from 2495 mamsl to 5002 mamsl. Hot springs may have originated from different hydrothermal systems (older for the Dari and Xilu hot springs, and younger for others). Our findings provide new insights into the possible spring water circulation and the origins of the NQ-QD Basin.

Data Availability

The geochemistry and isotope data (Tables 1–3) of the surface waters, saline, and hot springs in Nangqen and Qamdo Basin used to support the findings of this study are included within the article.

Conflicts of Interest

The authors declare that they have no conflicts of interest.

Acknowledgments

This research was funded by the Geological Resources and Geological Engineering Key Disciplines of Qinghai University (Grant No. 41250103) and the Qinghai Science and Technology Department (Grant No. 2021-ZJ-937Q). The fieldwork was supported by the Second Tibetan Plateau Scientific Expedition and Research Program (STEP), (Grant No. 2019QZKK0805). Sincere appreciation goes to Xu Jianxin and Zhai Ruyi for their help in the fieldwork and to Wang Bo for their suggestions and help during lab experiments. We also thank Ren Erfeng, Xia Chulin, Zhou Shumin, and other staff members of the Department of Geological Engineering, Qinghai University, for their support and assistance in our study.

References

[1] X. Daixiang, *Summarization of Mineral Resources in Tibet Autonomous Region (Chapter 7: Salt Mineral Resources)*, Regional Geological Survey Team of Tibetan Bureau of Geology and Mineral Resources, 1994.

[2] C. Kunpei and C. Shize, *Survey report of gypsum and salt spring in Qamdo, Tibet*, The Second Geological Brigade of the Ministry of Geology, Tibetan Exploration Group, 1980.

[3] K. Chen and S. Cao, *Survey Report of Gypsum and Saline Springs in Qamdo, Tibet*, Ministry of Geology second geological brigade Tibet exploration group, 1980.

[4] D. Xia, *Summary of Regional Mineral Resources in Tibet Autonomous Region (Chapter 7: Salt Minerals) (R)*, Tibet Bureau of Geology and Mineral Resources regional geological survey Brigade, 1994.

[5] N. Guo, Z. Liu, D. Nan, H. Sun, H. Li, and H. Zhao, "The characteristics and reservoir temperatures of hot springs in Jueyong, Qamdo, Xizang(Tibet)," *Geological Review*, vol. 66, pp. 499–509, 2020.

[6] N. Guo, H. Sun, and H. Li, "Hydrochemical characteristics of Jueyong hot spring in Tibet," *Geological Review*, vol. 65, pp. 21–23, 2019.

[7] J. L. Han, F. Q. Han, H. Syed-Asim, W. Y. Liu, N. Xiu-Qing, and Q. F. Mao, "Origin of boron and brine evolution in Saline Springs in the Nangqen Basin, southern Tibetan Plateau," *Geofluids*, vol. 2018, Article ID 1985784, 2018.

[8] X. Qin, H. Ma, X. Zhang et al., "Geochemical constraints on the origin and evolution of spring waters in the Changdu-Lanping-Simao Basin, southwestern China," *Acta Geologica Sinica*, vol. 93, pp. 1097–1112, 2019.

[9] X. Qin, H. Ma, X. Zhang et al., "Hydrochemical characteristics of salt spring and potassium-prospecting in Changdu Basin," *Journal of Salt Lake Research*, vol. 25, pp. 28–39, 2017.

[10] C. Ting, "Studyon the exploration and genesis of hot spring in Qamdo region BaSu County Bai Ma town," *Chengdu University of Technology*, pp. 1–78, 2014.

[11] C. Zhang, X. Li, J. Ma, C. Fu, and Z. Bai, *Formation Model of Geothermal Water in Chaya County, Tibet: Perspective from Hydrochemistry and Stable Isotopes Geoscience*, pp. 199–208, 2021.

[12] D. Cinti, L. Pizzino, N. Voltattorni, F. Quattrocchi, and V. Walia, "Geochemistry of thermal waters along fault segments in the Beas and Parvati valleys (north-west Himalaya, Himachal Pradesh) and in the Sohna town (Haryana), India," *Geochemical Journal*, vol. 43, pp. 65–76, 2009.

[13] S. Karimi, Z. Mohammadi, and N. Samani, "Geothermometry and circulation depth of groundwater in Semnan thermal springs, Northern Iran," *Environmental Earth Sciences*, vol. 76, p. 659, 2017.

[14] A. Rezaei, H. Javadi, M. Rezaeian, and S. Barani, "Heating mechanism of the Abgarm–Avaj geothermal system observed with hydrochemistry, geothermometry, and stable isotopes of thermal spring waters, Iran," *Environmental Earth Sciences*, vol. 77, p. 635, 2018.

[15] I. D. Clark and P. Fritz, *Environmental isotopes in hydrogeology*, CRC press, 1997.

[16] R. Clayton, I. Friedman, D. Graf, T. Mayeda, W. Meents, and N. Shimp, "The origin of saline formation waters: 1. Isotopic composition," *Journal of Geophysical Research*, vol. 71, pp. 3869–3882, 1966.

[17] H. Craig, "Isotopic variations in meteoric waters," *Science*, vol. 133, pp. 1702-1703, 1961.

[18] H. Tan, W. Zhang, J. Chen, S. Jiang, and N. Kong, "Isotope and geochemical study for geothermal assessment of the Xining basin of the northeastern Tibetan Plateau," *Geothermics*, vol. 42, pp. 47–55, 2012.

[19] H. Tan, Y. Zhang, W. Zhang, N. Kong, Q. Zhang, and J. Huang, "Understanding the circulation of geothermal waters in the Tibetan Plateau using oxygen and hydrogen stable isotopes," *Applied Geochemistry*, vol. 51, pp. 23–32, 2014.

[20] M. Paternoster, M. Liotta, and R. Favara, "Stable isotope ratios in meteoric recharge and groundwater at Mt. Vulture volcano, southern Italy," *Journal of Hydrology*, vol. 348, pp. 87–97, 2008.

[21] D. J. Qin, V. Jeffrey, and Turner and Pang, Z.H., "Hydrogeochemistry and groundwater circulation in the Xi'an geothermal field, China," *Geothermics*, vol. 34, pp. 471–494, 2005.

[22] M. P. Unterweger, B. M. Coursey, F. J. Shima, and W. B. Mann, "Preparation and calibration of the 1978 National Bureau of Standards tritiated water standards," *International Journal of Applied Radiation and Isotopes*, vol. 31, pp. 611–614, 1980.

[23] I. Cartwright and U. Morgenstern, "Using tritium to document the mean transit time and sources of water contributing to a chain-of-ponds river system: implications for resource protection," *Applied Geochemistry*, vol. 75, pp. 9–19, 2016.

[24] I. Cartwright and U. Morgenstern, "Using tritium and other geochemical tracers to address the "Old water paradox" in headwater catchments," *Journal of Hydrology*, vol. 563, pp. 13–21, 2018.

[25] C. Apollaro, G. Vespasiano, F. Muto, R. D. Rosa, D. Barca, and L. Marini, "Use of mean residence time of water, flowrate, and equilibrium temperature indicated by water geothermometers to rank geothermal resources. Application to the thermal water circuits of northern Calabria," *Journal of Volcanology & Geothermal Research*, vol. 328, pp. 147–158, 2016.

[26] C. Apollaro, G. Vespasiano, R. D. Rosa, and L. Marini, "Use of mean residence time and flowrate of thermal waters to evaluate the volume of reservoir water contributing to the natural discharge and the related geothermal reservoir volume. Application to northern Thailand hot springs," *Geothermics*, vol. 58, pp. 62–74, 2015.

[27] S. Chatterjee, U. K. Sinha, M. A. Ansari, H. V. Mohokar, and A. Dash, "Application of lumped parameter model to estimate mean transit time (MTT) of the thermal water using environmental tracer (3H): insight from Uttarakh and geothermal area (India)," *Applied Geochemistry*, vol. 94, pp. 1–10, 2018.

[28] L. Shevenell and F. Goff, "The use of tritium in groundwater to determine fluid mean residence times of Valles caldera hydrothermal fluids, New Mexico, USA," *Journal of Volcanology & Geothermal Research*, vol. 67, pp. 187–205, 1995.

[29] I. A. E. Agency, *Global network of isotopes in precipitation, WISER database*, 2016, January, 2016, http://www-naweb.iaea.org/napc/ih/IHS_resources_gnip.html.

[30] C. J. Eastoe, C. J. Watts, M. Ploughe, and W. E. Wright, "Future use of tritium in mapping pre-bomb groundwater volumes," *Ground Water*, vol. 50, pp. 87–93, 2011.

[31] Y. Bo, C. Liu, Y. Zhao, and L. Wang, "Chemical and isotopic characteristics and origin of spring waters in the Lanping–

Simao Basin, Yunnan, Southwestern China," *Geochemistry*, vol. 75, no. 3, pp. 287–300, 2015.

[32] I. Stober, J. Zhong, L. Zhang, and K. Bucher, "Deep hydrothermal fluid–rock interaction: the thermal springs of Da Qaidam, China," *Geofluids*, vol. 16, 2016.

[33] B. Ying, C. Liu, P. Jiao, Y. Chen, and Y. Cao, "Hydrochemical characteristics and controlling factors for waters' chemical composition in the Tarim Basin, Western China," *Chemie der Erde-Geochemistry-Interdisciplinary Journal for Chemical Problems of the Geosciences and Geoecology*, vol. 73, pp. 343–356, 2013.

[34] Y. Zhang, H. Tan, W. Zhang, H. Wei, and T. Dong, "Geochemical constraint on origin and evolution of solutes in geothermal springs in western Yunnan, China," *Geochemistry*, vol. 76, pp. 63–75, 2016.

[35] M. A. Ansari, H. V. Mohokar, A. Deodhar, N. Jacob, and U. K. Sinha, "Distribution of environmental tritium in rivers, groundwater, mine water and precipitation in Goa, India," *Journal of Environmental Radioactivity*, vol. 189, p. 120, 2018.

[36] S. Chatterjee, M. A. Gusyev, U. K. Sinha, H. V. Mohokar, and A. Dash, "Understanding water circulation with tritium tracer in the Tural-Rajwadi geothermal area, India," *Applied Geochemistry*, vol. 109, article 104373, 2019.

[37] E. Peters, A. Visser, B. K. Esser, and J. E. Moran, "Tracers reveal recharge elevations, groundwater flow paths and travel times on Mount Shasta, California," *Water*, vol. 10, p. 97, 2018.

[38] A. Rezaei, M. Rezaeian, and S. Porkhial, "The hydrogeochemistry and geothermometry of the thermal waters in the Mouil graben, Sabalan volcano, NW Iran," *Geothermics*, vol. 78, pp. 9–27, 2018.

[39] N. Yi, M. C. Castro, C. M. Hall, C. J. Poulsen, and P. Aron, "Groundwater sources in the island of Maui, Hawaii — a combined noble gas, stable isotope, and tritium approach," *Applied Geochemistry*, vol. 117, article 104587, 2020.

[40] W. Deng and H. Sun, "K-Ar age of the Cenozoic volcanic rocks in the Nangqen Basin, Qinghai Province and its geological significance," *Chinese Science Bulletin*, vol. 45, pp. 1015–1019, 2000.

[41] Z. Qi, Y. Li, C. Wang, T. Sun, and J. Zhang, "Organic geochemistry of the Paleocene-Eocene oil shales of the Gongjue formation, Nangqian basin, east-central Tibetan plateau," *Oil Shale*, vol. 34, pp. 1–14, 2017.

[42] D. Yang and P. Wang, "The Determinations of plateau age by 40Ar-39Ar dating on cenozoic calcalkalic trachytes of Nangqen basin, northern transverse mountains," *Contribution to the geology of the Qinghai-Xizang (Tibet)*, pp. 39–44, 1988.

[43] F. Han, Y. Chen, J. Han et al., "Boron isotope geochemical characteristics and its geological significances of high salinity salt springs in Nangqian Basin, Qinghai Province, China," *Acta Geoscientica Sinica*, vol. 37, pp. 723–732, 2016.

[44] W. M. Deng, H. J. Sun, and Y. Q. Zhang, "Petrogenesis of Cenozoic potassic volcanic rocks in the Nangqen basin," *Acta Geologica Sinica (English Edition)*, vol. 75, pp. 27–40, 2001.

[45] M. Wei, "Eogene ostracods from Nangqen in Qinghai.," *Contribution to the geology of the Qinghai-Xizang (Tibet)*, pp. 313–325, 1985.

[46] D. Yang and Wang., P., "The determinations of plateau age by $^{40}Ar/^{39}Ar$ dating on Cenozoic calc-alkalic trachytes of Nangqen Basin, northern transverse mountains," *Contribution to the Geology of the Qinghai-Xizang (Tibet) Plateau*, vol. 19, pp. 39–44, 1988.

[47] W. Deng, H. Sun, and Y. Zhang, "K·Ar age of the Cenozoic volcanic rocks in the Nangqen Basin, Qinghai Porvince and its geological signiifcance," *Chinese Science Bulletin*, vol. 45, pp. 1015–1019, 2000.

[48] Y. Jiang, S. Jiang, H. Ling, and B. Dai, "Low-degree melting of a metasomatized lithospheric mantle for the origin of Cenozoic Yulong monzogranite-porphyry, East Tibet: geochemical and Sr-Nd-Pb-Hf isotopic constraints," *Earth and Planetary Science Letters*, vol. 241, pp. 617–633, 2006.

[49] S. Hong Juan, D. Wan Ming, and Z. Yu Quan, "Petrogenesis of Cenozoic potassic volcanic rocks in Nangqen Basin," *Chinese Journal of Geology*, vol. 36, pp. 304–318, 2001.

[50] H. J. Sun, W. M. Deng, and Y. Q. Zhang, "Petrogeochemistry of the Cenozoic high-K alkaline volcanic rocks in the Nangqian Basin," *Geology Review*, vol. 145, pp. 958–965, 1999.

[51] G. Pan, Z. Chen, and X. Li, *Geological-Teological-Tectonic Evolution in the Eastem Testem Tethys*, Geological Publishing House, Beijing, 1997.

[52] W. Zhao, F. Tan, and M. Chen, "Sedimentary-tectonic evolution and hydrocarbon potential in the Qamdo Basin, eastern Xizang," *Sedimentary Geology and Tethyan Geology*, vol. 384, pp. 85–96, 2018.

[53] J. Deng, Q. Wang, G. Li, C. Li, and C. Wang, "Tethys tectonic evolution and its bearing on the distribution of important mineral deposits in the Sanjiang region, SW China," *Gondwana Research*, vol. 26, pp. 419–437, 2014.

[54] D. Du, J. Luo, and X. Li, "Sedimentary evolution and palaeogeography of the Qamdo block in Xizang," *Lithofacies palaeogeography*, vol. 17, pp. 1–17, 1997.

[55] Q. Lin, *Study on the Formation and Evolution Mechanisms of Underground Thermal Bittern in Yanjing County of Tibet*, Chengdu University of Technology, 2007.

[56] J. Duo, "The basic characteristics of the Yangbajing geothermal field-a typical high temperature geothermal system," *Engineering Science*, vol. 5, pp. 42–47, 2003.

[57] Q. Guo, Y. Wang, and W. Liu, "Major hydrogeochemical processes in the two reservoirs of the Yangbajing geothermal field, Tibet, China," *Journal of Volcanology and Geothermal Research*, vol. 166, pp. 255–268, 2007.

[58] Y. Wang, W. Fan, Y. Zhang, T. Peng, X. Chen, and Y. Xu, "Kinematics and 40Ar/39Ar geochronology of the Gaoligong and Chongshan shear systems, western Yunnan, China: implications for early Oligocene tectonic extrusion of SE Asia," *Tectonophysics*, vol. 418, pp. 235–254, 2006.

[59] Q. J. Yang, Y. G. Xu, X. L. Huang, and Z. Y. Luo, "Geochronology and geochemistry of granites in the Gaoligong tectonic belt western Yunnan: tectonic implications," *Acta Petrologica Sinica*, vol. 22, pp. 817–834, 2006.

[60] D. L. Zhong, *The Paleotethys Orogenic Belt in West of Sichuan and Yunnan*, Science Publishing House, Beijing, 1998.

[61] Y. Qu, K. Sun, and K. Chen, *Potash-Forming Rules and Prospect of Lower Tertiary in Lanping-Simao Basin*, Geological Publishing House, Yunnan. Beijing, 1998.

[62] Y. Sun and S. Sun, "The structure-paleohydrogeology and minerogenesis of Lanping-Simao basin," *Journal of Chengdu University of Technology*, vol. 3, p. 15, 1990.

[63] I. Metcalfe, "Tectonic framework and Phanerozoic evolution of Sundaland," *Gondwana Research*, vol. 19, pp. 3–21, 2011.

[64] I. Metcalfe, "Gondwana dispersion and Asian accretion: tectonic and palaeogeographic evolution of eastern Tethys," *Journal of Asian Earth Sciences*, vol. 66, pp. 1–33, 2013.

[65] A. Nair, "Possibilities of Liquid Scintillation Counting for Tritium Andradiocarbon Measurements in Natural Water," in *Proceedings of the Workshop on Isotope Hydrology*, pp. 41–56, Mumbai, 1983.

[66] K. Rozanski and M. Gröning, "Tritium assay in water samples using electrolytic enrichment and liquid scintillation spectrometry," in *Quantifying Uncertainty in Nuclear Analytical Measurements*, pp. 195–218, IAEA, Vienna, 2004.

[67] C. Taylor, "Present status and trends in electrolytic enrichment of lowlevel tritium in water," in *Methods of Low-level Counting and Spectrometry*, IAEA, Vienna, 1981.

[68] J. Horita, D. R. Cole, and D. J. Wesolowski, "The activity-composition relationship of oxygen and hydrogen isotopes in aqueous salt solutions: III. Vapor-liquid water equilibration of NaCl solutions to 350˚C," *Geochimica et Cosmochimica Acta*, vol. 59, pp. 1139–1151, 1995.

[69] J. Horita, D. J. Wesolowski, and D. R. Cole, "The activity-composition relationship of oxygen and hydrogen isotopes in aqueous salt solutions: I. Vapor-liquid water equilibration of single salt solutions from 50 to 100˚C," *Geochimica et Cosmochimica Acta*, vol. 57, pp. 2797–2817, 1993.

[70] J. Horita, D. J. Wesolowski, and D. R. Cole, "The activity-composition relationship of oxygen and hydrogen isotopes in aqueous salt solutions: II. Vapor-liquid water equilibration of mixed salt solutions from 50 to 100˚C and geochemical implications," *Geochimica Et Cosmochimica Acta*, vol. 57, no. 12, pp. 2797–2817, 1993.

[71] Q. Guo, Y. Wang, and W. Liu, "O, H, and Sr isotope evidences of mixing processes in two geothermal fluid reservoirs at Yangbajing, Tibet, China," *Environmental Earth Sciences*, vol. 59, pp. 1589–1597, 2010.

[72] P. Ala-Aho, C. Soulsby, O. S. Pokrovsky et al., "Using stable isotopes to assess surface water source dynamics and hydrological connectivity in a high-latitude wetland and permafrost influenced landscape," *Journal of Hydrology*, vol. 556, pp. 279–293, 2018.

[73] S. Kumar Joshi, S. P. Rai, R. Sinha et al., "Tracing groundwater recharge sources in the northwestern Indian alluvial aquifer using water isotopes (δ18O, δ2H and 3H)," *Journal of Hydrology*, vol. 559, pp. 835–847, 2018.

[74] L. A. Richards, D. Magnone, A. J. Boyce, M. J. Casanueva-Marenco, and D. A. Polya, "Delineating sources of groundwater recharge in an arsenic-affected Holocene aquifer in Cambodia using stable isotope-based mixing models," *Journal of Hydrology*, vol. 557, 2017.

[75] S. Santoni, F. Huneau, E. Garel et al., "Residence time, mineralization processes and groundwater origin within a carbonate coastal aquifer with a thick unsaturated zone," *Journal of Hydrology*, vol. 540, pp. 50–63, 2016.

[76] J. Liu, Y. Zhao, E. Liu, and D. Wang, "Discussion on the stable isotope time-space distribution law of China atmospheric precipitation site investigation," *Science and Technology*, vol. 3, pp. 34–39, 1997.

[77] J. Yu, H. Zhang, F. Yu, and D. Liu, "Oxygen isotopic composition of meteoric water in the eastern part of Tibet," *Geochimica*, vol. 2, pp. 113–121, 1980.

[78] C. Zhang, X. Li, J. Ma, C. Fu, and Z. Bai, "Formation model of geothermal water in Chaya County, Tibet: perspective from hydrochemistry and stable isotopes," *Geoscience*, vol. 35, pp. 1–14, 2020.

[79] I. Clark and P. Fritz, *Environmental Isotopes in Hydrogeology*, Lewis Publishers, Boca Raton, 1997.

[80] W. Dansgaard, "Stable isotopes in precipitation," *Tellus*, vol. 16, no. 4, pp. 436–468, 1964.

[81] Y. Yurtsever and J. Gat, *Atmospheric waters. In stable Isotope-Hydrology: deuterium and Oxygen-18 in the water cycle*, J. R. Gat and R. Gonfiantini, Eds., IAEA, Vienna, 1981.

[82] A. Longinelli and E. Selmo, "Isotopic composition of precipitation in Italy: a first overall map," *Journal of Hydrology*, vol. 270, pp. 75–88, 2003.

[83] P. Zhao, J. Dor, E. J. Xie, and J. Jin, "Strontium isotope data for thermal waters in selected high-temperature geothermal fields, China," *Acta Petrologica Sinica*, vol. 19, pp. 569–576, 2003.

[84] R. Zhang, *Application of isotope methods in hydrogeology*, pp. 8–13, 1978.

[85] F. J. Alcalá and E. Custodio, "Using the Cl/Br ratio as a tracer to identify the origin of salinity in aquifers in Spain and Portugal," *Journal of Hydrology*, vol. 359, pp. 189–207, 2008.

[86] S. N. Davis, D. O. Whittemore, and J. Fabryka-Martin, "Uses of chloride/bromide ratios in studies of potable water," *Groundwater*, vol. 36, pp. 338–350, 1998.

[87] J. Fabryka-Martin, D. O. Whittemore, S. N. Davis, P. W. Kubik, and P. Sharma, "Geochemistry of halogens in the Milk River aquifer, Alberta, Canada," *Applied Geochemistry*, vol. 6, pp. 447–464, 1991.

[88] J. T. Freeman, "E use of bromide and chloride mass ratios to di erentiate salt-dissolution and formation brines in shallow groundwaters of the Western Canadian Sedimentary Basin," *Hydrogeology Journal*, vol. 15, pp. 1377–1385, 2007.

[89] G. Rittenhouse, "Bromide in oil eld waters and its use in determining possibilities of origin of these waters," *American Association Petroleum Geology Bulletin*, vol. 51, pp. 2430–2440, 1967.

[90] J. C. Fontes, M. Yous, and G. B. Allison, "Estimation of long term, di use groundwater discharge in the northern Sahara using stable isotope pro les in soil water," *Journal of Hydrology*, vol. 86, pp. 315–327, 1986.

[91] H. B. Tan, W. D. Ma, and Ma, H.z. and Zhang, X., "Hydrochemical characteristics of brines and application to locating potassium in western Tarim Basin," *Geochimica*, vol. 33, pp. 152–158, 2004.

[92] Y. Lin, J. He, T. Wang, and M. Ye, "*Geochemical characteristics of potassium-rich brine in triassic Chengdu salt basin of Sichuan basin its prospects for brine tapping*," *Geology of Chemical Minerals*, vol. 24, pp. 72–84, 2002.

[93] J. Jiao, "Study on the regional salt- and potash-forming in Jurassic strata," China University of Geosciences, Beijing, 2013, PhD Thesis.

[94] W. F. Giggenbach, "Chemical techniques in geothermal exploration," in *Application of Geochemistry in Geothermal Reservoir Development*, F. D'Amore, Ed., pp. 119–142, UNITAR/UNDP publication, Rome, 1991.

[95] K. K. Turekian and K. H. Wedepohl, "Distribution of the elements in some major units of the Earth's crust," *Geological Society of America Bulletin*, vol. 72, pp. 175–192, 1961.

[96] T. K. Lowenstein and F. Risacher, "Closed basin brine evolution and the influence of Ca–Cl inflow waters: Death Valley and Bristol Dry Lake California, Qaidam Basin, China, and

Salar de Atacama, Chile," *Aquatic Geochemistry*, vol. 15, pp. 71–94, 2009.

[97] W. A. Deer, R. A. Howie, and J. Zussman, *An Introduction to the Rock Forming Minerals*, Longman Group, London, UK, 1966.

[98] J. Makni, S. Bouri, and H. B. Dhia, "Hydrochemistry and geothermometry of thermal groundwater of southeastern Tunisia (Gabes region)," *Arabian Journal of Geosciences*, vol. 6, pp. 2673–2683, 2013.

[99] D. Sanliyuksel and A. Baba, "Hydrogeochemical and isotopic composition of a low temperature geothermal source in Northwest Turkey: case study of Kirkgecit geothermal area," *Environmental Earth Sciences*, vol. 62, pp. 529–540, 2011.

[100] A. Yousafzai, Y. Eckstein, and P. S. Dahl, "Hydrochemical signatures of deep groundwater circulation in a part of the Himalayan foreland basin," *Environmental Earth Sciences*, vol. 59, pp. 1079–1098, 2010.

[101] S. Arnorsson and J. Gerardo-Abaya, "Isotopic and chemical techniques in geothermal exploration, development and use," in *Geochemistry, Groundwater and Pollution*, A. CAJ and D. Postma, Eds., pp. 1–647, International Atomic Energy Agency, Rotterdam, 2nd edition, 2000.

[102] J. Wang, L. Xiong, and Z. Pang, "Low-medium temperature geothermal system of convective type," Science Press, Beijing, 1993.

[103] W. F. Giggenbach, "Geothermal solute equilibrium, derivation of Na–K–mg–ca geoindicators," *Geochimica et Cosmochimica Acta*, vol. 52, pp. 2749–2765, 1988.

[104] R. O. Fournier, "Application of water geochemistry to geothermal exploration and reservoir engineering," in *Geothermal Systems: Principles and Case Histories*, L. Rybach and L. J. P. Muffler, Eds., pp. 109–143, John Wiley and Sons Ltd., New York, 1981.

[105] M. A. Gusyev, U. Morgenstern, M. K. Stewart et al., "Application of tritium in precipitation and baseflow in Japan: a case studyof groundwater transit times and storage in Hokkaido watersheds," *Hydrology and earth system sciences*, vol. 20, pp. 3043–3058, 2016.

[106] L. L. Lucas and M. P. Unterweger, "Comprehensive review and critical evaluation of the half-life of tritium," *Journal of Research of the National Institute of Standards & Technology*, vol. 105, pp. 541–549, 2000.

[107] M. A. Ansari, S. Sharma, U. S. Kumar, S. Chatterjee, and U. Low, "*Hydrogeological controls of radon in a few hot springs in the Western Ghats at Ratnagiri District in Maharashtra, India*," *Current Science*, vol. 107, no. 9, p. 107, 2014.

[108] I. Cartwright and U. Morgenstern, "Constraining groundwater recharge and the rate of geochemical processes using tritium and major ion geochemistry: ovens catchment, Southeast Australia," *Journal of Hydrology*, vol. 475, pp. 137–149, 2012.

[109] I. Cartwright and U. Morgenstern, "Using tritium to document the mean transit time and sources of water distributing to a chain-of-ponds river system: implications for resource protection," *Applied Geochemistry*, vol. 75, pp. 9–19, 2016.

[110] J. A. Izbicki, J. Radyk, and R. L. Michel, "Water movement through a thick unsaturated zone underlying an intermittent stream in the western Mojave Desert, southern California, USA," *Journal of Hydrology*, vol. 238, pp. 194–217, 2000.

[111] A. Sawodni, A. Pazdur, and J. Pawlyta, "Measurements of tritium radioactivity in surface water on the Upper Silesia region," *Geochronometria*, vol. 18, pp. 23–28, 2000.

[112] C. V. Tadros, C. E. Hughes, J. Crawford, S. E. Hollins, and R. Chisari, "Tritium in Australian precipitation: a 50 year record," *Journal of Hydrology*, vol. 513, pp. 262–273, 2014.

[113] T. J. Yasunari and K. Yamazaki, "Impacts of Asian dust storm associated with the stratosphere-to-troposphere transport in the spring of 2001 and 2002 on dust and tritium variations in Mount Wrangell ice core, Alaska," *Atmospheric Environment*, vol. 43, pp. 2582–2590, 2009.

[114] H. Yangui, I. Abidi, K. Zouari, and K. Rozanski, "Deciphering groundwater flow between the complex terminal and Plioquaternary aquifers in Chott Gharsa plain (southwestern Tunisia) using isotopic and chemical tools," *Hydrological Sciences Journal*, vol. 57, pp. 967–984, 2012.

[115] W. F. Giggenbach, "Isotopic shifts in waters from geothermal and volcanic systems along convergent plate boundaries and their origin," *Earth and planetary science letters*, vol. 113, pp. 495–510, 1992.

[116] F. W. Schwartz, *Fundamentals of Ground Water*, Wiley, 2003.

[117] C. Zongyu, Q. Jixiang, and Z. Zhaoji, *Isotope Hydrogeology Method Applied in the Typical Northern Basin*, Science Press, Beijing, 2010.